

Characterizing correlation within multipartite quantum systems via local randomized measurements

Zhenhuan Liu,^{1,*} Pei Zeng,^{2,1,†} You Zhou,^{3,4,‡} and Mile Gu^{3,4,§}

¹Center for Quantum Information, Institute for Interdisciplinary Information Sciences, Tsinghua University, Beijing 100084, China

²CAS Center for Excellence in Quantum Information and Quantum Physics, University of Science and Technology of China, Hefei, Anhui 230026, China

³Nanyang Quantum Hub, School of Physical and Mathematical Sciences, Nanyang Technological University, Singapore 637371

⁴Centre for Quantum Technologies, National University of Singapore, 3 Science Drive 2, 117543 Singapore

Given a quantum system on many qubits split into a few different parties, how many total correlations are there between these parties? Such a quantity, aimed to measure the deviation of the global quantum state from an uncorrelated state with the same local statistics, plays an important role in understanding multipartite correlations within complex networks of quantum states. Yet, the experimental access of this quantity remains challenging as it tends to be non-linear, and hence often requires tomography which becomes quickly intractable as dimensions of relevant quantum systems scale. Here, we introduce a much more experimentally accessible quantifier of total correlations, which can be estimated using only single-qubit measurements. It requires far fewer measurements than state tomography, and obviates the need to coherently interfere multiple copies of a given state. Thus we provide a tool for proving multipartite correlations that can be applied to near-term quantum devices.

I. INTRODUCTION

The preparation of highly correlated quantum states across many qubits is essential for advanced quantum information processing [1–3]. Yet, in the noisy intermediate-scale quantum (NISQ) era, techniques for doing so are not necessarily reliable. Consequently, there is surging interest in quantum benchmarking [4, 5] — identifying efficient means of verifying what a quantum computer is doing compared to what it is meant to do. Of these, an analysis of how many correlations exist across many qubits faces significant challenges owing to the exponentially growing size of Hilbert space. This is especially true when there is no prior information regarding how the state is prepared.

One key amount of common interest is the total correlation within a multipartite quantum system [3, 6]. Consider a joint quantum system consisting of k subsystems $\{g_1, g_2, \dots, g_k\}$, where each subsystem g_i has local statistics specified by respective density operator ρ_i . The joint system would be said to have no correlation if the joint state obeys $\rho = \bigotimes_{i=1}^k \rho_i$, such that the global statistics is simply the product of its marginals. A state then possesses correlations if there exists deviation from this tensor product. A common measure of such deviation is the relative entropy, resulting in the quantifier $S(\rho \| \bigotimes_{i=1}^k \rho_i) = \sum_i S(\rho_i) - S(\rho)$, where $S(\cdot)$ represents the von Neumann entropy. The quantity has found applications in quantum thermodynamics [7] and many-body

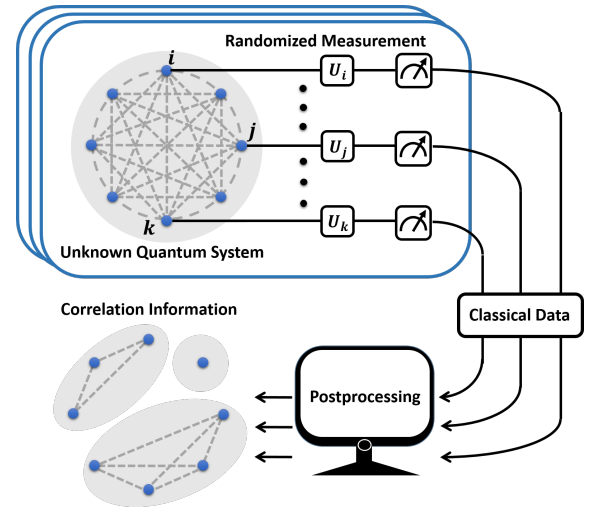


FIG. 1. Illustration of the main idea. We present a protocol to measure the total correlation of an unknown multipartite quantum state in any partition. We perform qubitwise local randomized measurements on sequentially prepared states and thus obtain the classical measurement data. Using tailored data postprocessing strategies, the correlation information with respect to any chosen partition can be extracted.

physics [8, 9], and the characterization of genuine multipartite correlation [10–12]. Nevertheless, the quantity remains difficult to access in practical experiments due to its inherent nonlinearity. Most approaches would require either interacting multiple copies of ρ or state tomography, tasks that can be prohibitive if ρ already presents the most challenging state one can synthesize on NISQ devices.

Here, we propose a quantifier of the total correlation

* liu-zh20@mails.tsinghua.edu.cn

† peizeng.phy@gmail.com

‡ zyqphy@gmail.com

§ mgu@quantumcomplexity.org

— *correlation overlap* — whose technological accessibility is much closer to the synthesis of ρ itself. In particular, our protocol only requires repeated synthesis of the same ρ , together with local (qubitwise) random unitary evolution and computational measurements (see Fig. 1). Specifically, we show that the *correlation overlap* can be obtained by postprocessing the measurement data and the amount of data required is much less than the traditional quantum tomography. Meanwhile, the quantity itself maintains its operational meaning as a quantifier of total correlations, and can also be immediately adapted to measure how close candidate systems are to the maximally entangled.

II. DEFINITION

Recall that if a k -partite quantum state ρ is uncorrelated, it can be written as $\bigotimes_{i=1}^k \rho_i$ with $\rho_i = \text{tr}_{\bar{i}}(\rho)$ being the reduced density matrix of the i -th subsystem. Normally the relative entropy is adopted to quantify the distance between them [3, 6]. The von Neumann entropy involved can be in principle acquired by the quantum state tomography, which is already challenging for systems with more than ten qubits. Thus, in order to make the measurement protocol scalable, one needs to avoid state tomography [13]. Alternative entropy functions such as Rényi entropy can be obtained by measuring the purity of the state [14–16]. However, Rényi entropy can violate the subadditivity [2, 17], which makes it nonideal for quantifying total correlation. Alternative approaches include uses of witnesses [18, 19] to detect the presence of certain correlations [20–23]. These witnesses are typically tailored for specific classes of states (e.g. [23, 24]) and are generally ineffective when applied to states without the preparation information [25–27].

Here we quantify the total correlation based on the fidelity between a given state ρ and its marginals as follows:

$$C(\rho) = -\log \mathcal{F} \left(\rho, \bigotimes_{i=1}^k \rho_i \right), \quad (1)$$

with the fidelity [28] being

$$\mathcal{F} \left(\rho, \bigotimes_{i=1}^k \rho_i \right) = \frac{\text{tr} \left(\rho \bigotimes_{i=1}^k \rho_i \right)}{\sqrt{\text{tr}(\rho^2) \left[\prod_{i=1}^k \text{tr}(\rho_i^2) \right]}}. \quad (2)$$

Notice that k is not necessarily the number of qubits, but the number of subsystems under some partition. In Appendix B, we show that such total correlation measure satisfies certain key properties, such as faithfulness, no change under local unitary transformation, and additivity under tensor product. By taking the minimization on all possible bipartitions, one can also generalize it to quantify genuine multipartite correlation. We remark

that other fidelity measures [28] could also be adapted to define the total correlation where the measurability is the main concern.

The denominator of Eq. (2) is composed of a few purity terms, and there already exist effective methods to measure them [16, 29]. The main contribution of this work is that we develop a protocol to effectively measure the numerator

$$T_k := \text{tr} \left(\rho \bigotimes_{i=1}^k \rho_i \right) \quad (3)$$

based on randomized measurements [16, 30, 31]. We denote T_k as the *correlation overlap* (CRO), which is directly relative to the Hilbert-Schmidt distance

$$D_{\text{HS}} \left(\rho, \bigotimes_{i=1}^k \rho_i \right) = \text{tr}(\rho^2) + \prod_{i=1}^k \text{tr}(\rho_i^2) - 2T_k. \quad (4)$$

When ρ is a low-rank state [32], such quantity can offer a tight bound of the trace distance between ρ and its marginals, which can be further applied in the quantum independence testing [33]. In addition, we also discuss the application of bipartite CRO in bipartite entanglement detection, and leave it in Appendix C.

III. EFFICIENT ESTIMATION PROTOCOLS

We now show that the total correlation defined in the previous section can be effectively estimated, irrelevant of the party number k . For simplicity of discussion, take the tripartite state ρ_{ABC} as an example. Following the definition in Sec. II, the essential quantity one needs to evaluate is the tripartite CRO

$$T_3 = \text{tr} [\rho_{ABC} (\rho_A \otimes \rho_B \otimes \rho_C)]. \quad (5)$$

The difficulty to measure T_3 lies in that it is a nonlinear function of ρ_{ABC} and thus cannot be obtained by measuring the observable on a single-copy state. In fact, given four identical states $\rho_{ABC}^{\otimes 4}$, one can make a joint measurement among these copies [29],

$$\begin{aligned} T_3 &= \text{tr} \{ S_A \otimes S_B \otimes S_C [\rho_{ABC} \otimes (\rho_A \otimes \rho_B \otimes \rho_C)] \} \\ &= \text{tr} \left[S_A^{(1,2)} \otimes S_B^{(1,3)} \otimes S_C^{(1,4)} (\rho_{ABC}^{\otimes 4}) \right]. \end{aligned} \quad (6)$$

Here $S_A^{(1,2)}$ is the SWAP operator acting on the Hilbert space of the first two copies of subsystem A , $\mathcal{H}_A^1 \otimes \mathcal{H}_A^2$, and acts trivially on the last two copies, $S_A^{(1,2)} |\psi\rangle_A^1 |\phi\rangle_A^2 = |\phi\rangle_A^1 |\psi\rangle_A^2$. And similarly for the other SWAP operators $S_B^{(1,3)}$ and $S_C^{(1,4)}$ (see Fig. 2(c) for an illustration).

This kind of measurement in general demands the preparation of identical copies of the state ρ , and the joint measurements across the distinct copies, which is possible for the one-dimensional system and the few parties case, for example, $k = 2$ [14, 15]. However, it is

very challenging for the higher-dimensional system and for the number of parties k being not small. In the following, we develop a measurement protocol based on randomized measurements [16, 30, 31, 34], which only needs the preparation of singlecopies of the state ρ . Randomized measurements find applications not only in quantum information, like entanglement negativity extraction [35–37], entanglement detection [38–42], Fisher information quantification [43, 44], and quantum certification [45–47], but also in quantum many-body physics [48–51].

Global Measurement Protocol – We first propose a means to measure CRO using random unitary gates that act globally on each system. This protocol can then be subsequently modified to use only local unitary gates on each qubit with a modest sacrifice in error scaling. Our global measurement protocol works as follows: Sample and operate random unitary $U = \bigotimes_{i=1}^k U_{g_i}$ on each subsystem g_i for the total k -partite system, independently, and then conduct computational basis measurement $|s\rangle = |s_{g_1}, s_{g_2}, \dots, s_{g_k}\rangle$ in a sequential manner. After sufficient repeating of the preparation and measurement, one can get the estimation of the conditional probability

$$\Pr\left(s_{g_1}, s_{g_2}, \dots, s_{g_k} \left| \bigotimes_{i=1}^k U_{g_i}\right.\right) = \langle s | U \rho U^\dagger | s \rangle \quad (7)$$

and also its marginals $\Pr(s_{g_i} | U_{g_i})$ for the i -th subsystem. The target quantity CRO T_k , can be written as the postprocessing of these conditional probabilities shown in Proposition 1, and we summarize the protocol in Algorithm 1.

Algorithm 1 Global Measurement Protocol for T_k

Input: $N_U \times N_M$ sequentially prepared ρ

Output: Probability distribution of the measurement outcomes conditioned on the evolution unitary

$$\Pr\left(s_{g_1}, s_{g_2}, \dots, s_{g_k} \left| \bigotimes_{i=1}^k U_{g_i}\right.\right) \text{ in Eq. (7).}$$

- 1: **for** $i = 1$ **to** N_U **do**
 - 2: Randomly pick a unitary matrix $U = \bigotimes_{i=1}^k U_{g_i}$, with each $U_{g_i} \in \mathcal{H}_{g_i}$ sampled uniformly from the unitary 2-design ensemble.
 - 3: Operate U on ρ to get $U \rho U^\dagger$.
 - 4: **for** $j = 1$ **to** N_M **do**
 - 5: Measure $U \rho U^\dagger$ in the computational basis $\{|s\rangle = |s_{g_1}, s_{g_2}, \dots, s_{g_k}\rangle\}$.
 - 6: Record the measurement results.
 - 7: **end for**
 - 8: Estimate the probability and its marginals in Eq. (7).
 - 9: **end for**
 - 10: Do the data postprocessing given in Proposition 1 for T_k .
-

Proposition 1. For a k -partite state ρ , the CRO T_k defined in Eq. (3), can be evaluated by postprocessing the measurement data, i.e., averaging the multiplication of the total and the marginal probabilities under the random

unitary evolution as follows:

$$T_k = \sum_{s, s'} \mathbb{E}_U \left[\Pr(s|U) \prod_{i=1}^k X_{g_i}(s_{g_i}, s'_{g_i}) \Pr(s'_{g_i} | U_{g_i}) \right], \quad (8)$$

with the function

$$X_{g_i}(s_{g_i}, s'_{g_i}) = -(-d_{g_i})^{\delta_{s_{g_i}, s'_{g_i}}}, \quad (9)$$

where d_{g_i} is the dimension of the i -th subsystem g_i , and \mathbb{E}_U denotes averaging over unitary 2-design ensembles on each subsystem g_i independently.

The detailed proof is left in Appendix D2. The intuition is that by multiplying the probabilities in the post-processing, one can *virtually* get a few copies of ρ . Then by averaging on the random unitary, one can further generate permutation operators among virtual copies.

Here we sketch the proof outline using Fig. 2 for the T_3 of the tripartite state ρ_{ABC} . In Fig. 2(a), the conditional probabilities are multiplied, and the box labels the classical function $X_g(s_g, s'_g)$ with $g \in \{A, B, C\}$ for the subsystem. In Fig. 2(b), by using the cyclic property of the trace, we can effectively put the random unitary on the operator $X_g = \sum_{s_g, s'_g} X_g(s_g, s'_g) |s_g, s'_g\rangle \langle s_g, s'_g|$. In Fig. 2(c), we average on the unitary ensemble to generate a SWAP operator by the identity [31, 52],

$$\Phi^2(X_g) := \mathbb{E}_{U_g \in \mathcal{E}} [U_g^{\otimes 2} X_g U_g^{\dagger \otimes 2}] = S_g. \quad (10)$$

We denote this average on the two-copy Hilbert space as the “twirling” channel $\Phi^2(\cdot)$. Note that the unitary ensemble \mathcal{E} need not be the Haar measure, and any unitary 2-design ensemble (such as the Clifford group [53, 54]) is sufficient, which is more practical compared with the previous work by some of us [36]. If one naively generalizes the protocol there to measure the k -partite CRO, a $(k+1)$ -design ensemble is needed. Unitary t -design with $t \geq 4$ is still poorly understood [55], and the generation of these ensembles would need deep quantum circuit, which is quite impractical compared to the current protocol.

In real experiments, the sampling time N_U and the measurement time N_M as shown in Algorithm 1 are both finite; the postprocessing will be more delicate compared to Eq. (8) which corresponds to the case where N_U and N_M are infinite. We show how to construct an unbiased estimator for the scenario with finite N_U and N_M in Sec. IV. We remark that our protocol measures the fidelity of the state to its marginal, not with an unrelated state as in Ref. [45]. By adequately utilizing the marginal distributions, our postprocessing shown in Sec. IV needs less state samples and thus is more efficient than directly applying the former one, say Ref. [45]. Our protocol can be further generalized to local gate version, as discussed in the next section.

Local Measurement Protocol – We can further simplify the procedure above so that it makes use of only

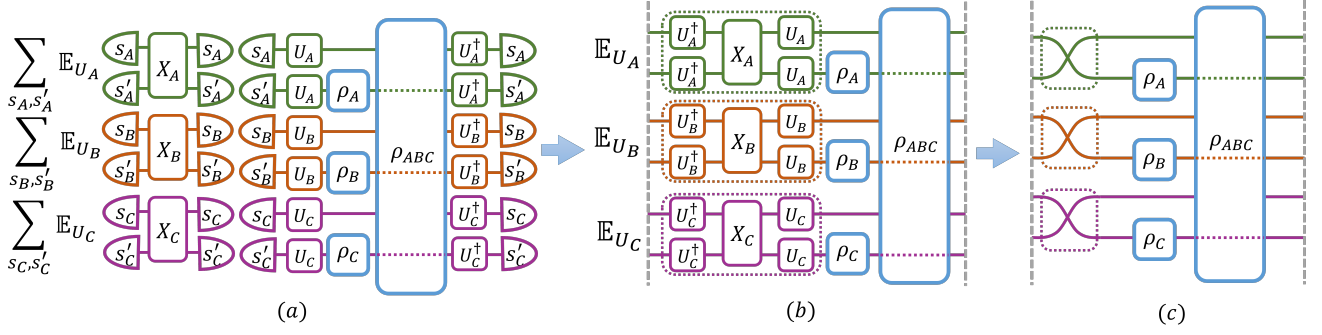


FIG. 2. Diagrammatic illustration of the proof of Proposition 1. Here, for simplicity, we take the tripartite state as an example. (a) is the diagram representation of Eq. (8). The small half circles with s, s' inside represent the computational basis measurement. The dashed lines indicate that ρ_{ABC} is not connected to $\rho_A \otimes \rho_B \otimes \rho_C$. In (b), we use the cyclic property of the trace formula to put the random unitary evolution on X_g , for $g \in \{A, B, C\}$, defined in Eq. (9). The vertical gray dashed lines denote the periodic boundary condition, i.e., the trace. The colored dashed boxes are twofold twirling channels acting on X_g , which equal to the SWAP operators as shown in Eq. (10). As a result, we recover T_3 in (c) with these SWAP operators represented by the “X”-shape cross in each dashed box, with the formula given in Eq. (6).

single-qubit random gates. Specifically, the global measurement protocol involves the need to sample random unitary on each subsystem, which may contain several qubits. This is challenging even for the moderate subsystem size. In contrast, the following local measurement protocol only involves random single-qubit Pauli measurement.

Recall that the essence of the global measurement protocol is to construct “virtual” SWAP operators across different copies in Eq. (6) by data postprocessing shown in Proposition 1. In fact, SWAP operator is factorizable. The big SWAP operator S acting on n -qubit pairs $\mathcal{H}_2^{\otimes n} \otimes \mathcal{H}_2^{\otimes n}$, can be decomposed as $S = \bigotimes_{l=1}^n S_l$, with S_l the small SWAP operator for the l -th qubit pair (see Fig. 3 for an illustration). This fact enlightens us to substitute the random unitary, say U_A (also U_B and U_C) in Fig. 2, to the tensor product form $U_A = \bigotimes_{l=1}^{n_A} U_l$, where each single-qubit unitary U_l is from the 2-design ensemble independently, similar for other subsystems B and C . Correspondingly, the postprocessing function $X_g(s_g, s'_g)$ in Eq. (9) is modified to the multiplication of local functions as shown in Eq. (13).

For the general k -partite state ρ , suppose it contains $n = \sum_{i=1}^k n_{g_i}$ qubits with i -th party having n_{g_i} qubits. We denote the computational basis as the n -bit binary vector $|\vec{s}\rangle = |s_1, s_2, \dots, s_n\rangle$, $s_l = 0/1$, and the state restricted on the i -th party as $|\vec{s}_{g_i}\rangle$. By modifying the global protocol in Algorithm 1, the local measurement protocol of CRO T_k is shown in Algorithm 2, and now we aim to obtain the following conditional probability

$$\Pr \left(s_1, s_2, \dots, s_n \left| \bigotimes_{l=1}^n U_l \right. \right) \quad (11)$$

and its marginals $\Pr(\vec{s}_{g_i} | U_{g_i})$ with $U_{g_i} = \bigotimes_{l \in g_i} U_l$. The data postprocessing is summarized in Proposition 2.

Proposition 2. *Given a k -partite state ρ , the CRO T_k defined in Eq. (3), can be evaluated by postprocessing the*

measurement data, i.e., averaging the multiplication of the total and the marginal probabilities under the single-qubit random unitary evolution as follows.

$$T_k = \sum_{\vec{s}, \vec{s}'} \mathbb{E}_U \left[\Pr(\vec{s}' | U) \prod_i^k \tilde{X}_{g_i}(\vec{s}_{g_i}, \vec{s}'_{g_i}) \Pr(\vec{s}_{g_i} | U_{g_i}) \right] \quad (12)$$

with the function

$$\tilde{X}_{g_i}(\vec{s}_{g_i}, \vec{s}'_{g_i}) := \prod_{l \in g_i} X_l(s_l, s'_l) \quad (13)$$

where X_l is defined in Eq. (9) with $d_l = 2$, and \mathbb{E}_U denotes averaging $U = \bigotimes_{l=1}^n U_l$ over unitary 2-design ensembles on each qubit independently.

Proposition 2 can be proved following the proof of Proposition 1, and the proof is left to Appendix D 3.

Algorithm 2 Local Measurement Protocol for T_k

Input: $N_U \times N_M$ sequentially prepared ρ
Output: Probability distribution of the measurement outcomes conditioned on the evolution unitary

$$\Pr \left(s_1, s_2, \dots, s_n \left| \bigotimes_{l=1}^n U_l \right. \right) \text{ in Eq. (11).}$$

- 1: **for** $i = 1$ **to** N_U **do**
 - 2: Randomly pick a unitary matrix $U = \bigotimes_{l=1}^n U_l$, with each $U_l \in \mathcal{H}_l$ on the l -th qubit sampled uniformly from the unitary 2-design ensemble.
 - 3: Operate U on ρ to get $U\rho U^\dagger$.
 - 4: **for** $j = 1$ **to** N_M **do**
 - 5: Measure $U\rho U^\dagger$ in the computational basis $\{|s\rangle = |s_1, s_2, \dots, s_n\rangle\}$.
 - 6: Record the measurement results.
 - 7: **end for**
 - 8: Estimate the probability and its marginals in Eq. (11).
 - 9: **end for**
 - 10: Do the data postprocessing given in Proposition 2 for T_k .
-

Besides the practicality of the local measurement protocol, another advantage is that the measurement procedure and the postprocessing procedure are decoupled. In particular, one can choose to study the correlation for any partition of the system or the correlation information restricted on some subsystems in parallel, by only changing the postprocessing function.

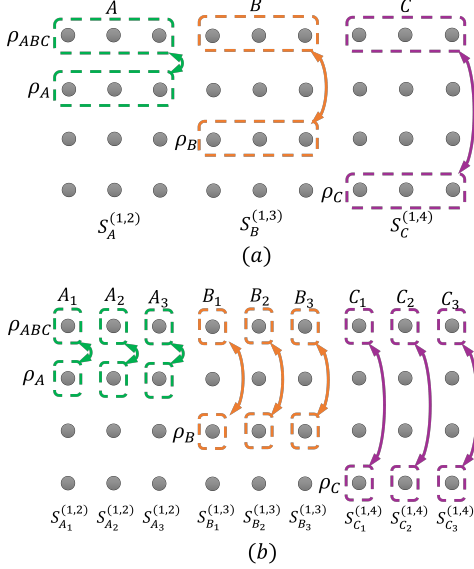


FIG. 3. Here we provide a graphical example explaining how the global and local methods work. ρ_{ABC} is a nine-qubit three-partite quantum state with each party containing three qubits. The curved lines with arrows in both ends denote SWAP operators. In global method (a), three-qubit SWAP operators are constructed using three-qubit random unitary matrix U_A , U_B , and U_C . While in local method (b), the three-qubit SWAP operators are decomposed into a tensor product of single-qubit SWAP operators, which can be constructed using single-qubit random unitary gates. Each colored dashed box represents a unitary 2-design.

IV. STATISTICAL ANALYSIS

In practical situations, the sampling times of the random unitary matrices N_U , and the number of the projective measurement N_M under a given unitary are both finite. The multiplication of them, $N_U N_M$, quantifies

how many copies of ρ in total one needs to prepare in sequence. In this section, for clarity, we focus on the tripartite CRO in Eq. (5) and construct an unbiased estimator for it. We then analyze the variance of the estimator in this finite sampling scenario. The scaling of the variance respective to N_U , N_M and D characterizes the sample complexity of our protocol. Similar analysis works for the cases of general k -partite CRO. We use $|s\rangle = |s_A, s_B, s_C\rangle$ to denote the computational basis of $\mathcal{H} = \mathcal{H}_A \otimes \mathcal{H}_B \otimes \mathcal{H}_C$, where the total dimension is $D = d_A d_B d_C$. In the following, we first illustrate the estimation protocol with global unitary evolution, and then proceed to show how this can be converted to the one with the single-qubit measurements.

To construct an unbiased estimator, we first note that the postprocessing expression in Eq. (8) can be equivalently written as 4-time multiplication of the probability distribution,

$$T_3 = \sum_{\mathbf{s}_A, \mathbf{s}_B, \mathbf{s}_C} X_A^{(1,2)}(s_A^1, s_A^2) X_B^{(1,3)}(s_B^1, s_B^3) X_C^{(1,4)}(s_C^1, s_C^4) \times \mathbb{E}_U \left[\prod_{i=1}^4 \Pr(s_A^i, s_B^i, s_C^i | U_A, U_B, U_C) \right], \quad (14)$$

where we denote $\mathbf{s}_A = (s_A^1, s_A^2, s_A^3, s_A^4)$ as a 4-dit string with $s_A^i \in \{0, 1, \dots, d_A - 1\}$, similar for \mathbf{s}_B and \mathbf{s}_C . $X_A^{(1,2)}(s_A^1, s_A^2)$ is the function in Eq. (9) restricted on the first two indices, similar for $X_B^{(1,3)}(s_B^1, s_B^3)$ and $X_C^{(1,4)}(s_C^1, s_C^4)$.

In Algorithm 1, one samples N_U times of $U = U_A \otimes U_B \otimes U_C$ to perform experiments. For the t -th round of unitary sampling, one repeats the preparation and measurement for N_M times. For the i -th time of measurement, we define a matrix-valued random variable

$$\hat{r}_U(i) = |\hat{s}_U(i)\rangle \langle \hat{s}_U(i)|, \quad (15)$$

where $\hat{s}_U(i)$ is a classical random variable with the conditional probability

$$\Pr(s|U) = \langle s|U\rho_{ABC}U^\dagger|s\rangle, \quad (16)$$

to record the measurement result s . For each random unitary choice, one finally gets N_M independent samples $\{\hat{r}_U(i)\}_{i=1}^{N_M}$. We then construct an estimator for T_3 as follows

$$\begin{aligned} \hat{M}(t) &= \binom{N_M}{4}^{-1} \sum_{1 \leq i < j < k < l \leq N_M} \text{tr} \{ Q_3 [\hat{r}_U(i) \otimes \hat{r}_U(j) \otimes \hat{r}_U(k) \otimes \hat{r}_U(l)] \} \\ &= \binom{N_M}{4}^{-1} \sum_{1 \leq i < j < k < l \leq N_M} X_A^{(1,2)}(\hat{s}_U(i), \hat{s}_U(j)) X_B^{(1,3)}(\hat{s}_U(i), \hat{s}_U(k)) X_C^{(1,4)}(\hat{s}_U(i), \hat{s}_U(l)), \end{aligned} \quad (17)$$

with

$$Q_3 := \left(X_A^{(1,2)} \otimes I_A^{(3,4)} \right) \otimes \left(X_B^{(1,3)} \otimes I_B^{(2,4)} \right) \otimes \left(X_C^{(1,4)} \otimes I_C^{(2,3)} \right) \quad (18)$$

being an observable on $\mathcal{H}^{\otimes 4}$. $\hat{M}(t)$ is an unbiased esti-

mator in the sense that $\mathbb{E}_{U,s} [\hat{M}(t)] = T_3$, with the expectation value taken for all random U and measurement outputs. Since the estimators $\{\hat{M}(t)\}_{t=1}^{N_U}$ are independent and identically distributed, the final estimator is defined as $\hat{M} = \frac{1}{N_U} \sum_{t=1}^{N_U} \hat{M}(t)$, which is naturally unbiased.

In the local measurement protocol, the unitaries on subsystems A , B and C are substituted to products of the random unitaries on qubits. To construct the unbiased estimator for the local protocol, accordingly the postprocessing matrix Q in Eq. (18) should be adjusted to

$$Q_{3,\text{loc}} := \left(\tilde{X}_A^{(1,2)} \otimes I_A^{(3,4)} \right) \otimes \left(\tilde{X}_B^{(1,3)} \otimes I_B^{(2,4)} \right) \otimes \left(\tilde{X}_C^{(1,4)} \otimes I_C^{(2,3)} \right) \quad (19)$$

with $\tilde{X}_A^{(1,2)} = \bigotimes_{i=1}^{n_A} X_{A_i}^{(1,2)}$ the product of the qubitwise X operator. Similar as in Eq. (17), one can construct the final unbiased estimator $\hat{M}_L = \frac{1}{N_U} \sum_{t=1}^{N_U} \hat{M}_L(t)$.

To construct the unbiased estimator for T_k , one just needs to extend the definition of Q_3 and $Q_{3,\text{loc}}$ to the k -partite scenario

$$Q_k := \bigotimes_{i=2}^{k+1} \left(X_{g_i}^{(1,i)} \otimes I_{g_i}^{\overline{(1,i)}} \right), \quad (20)$$

$$Q_{k,\text{loc}} := \bigotimes_{i=2}^{k+1} \left(\tilde{X}_{g_i}^{(1,i)} \otimes I_{g_i}^{\overline{(1,i)}} \right),$$

where $\overline{(1,i)}$ is the complementary set of $(1,i)$ of $\{1, 2, \dots, k+1\}$. We further give the following result on the variance of these constructed estimators for T_k .

Proposition 3. *In the regime $D \gg N_M \gg k$, the variance of the unbiased estimators \hat{M} and \hat{M}_L for the k -partite CRO show the following scaling:*

$$\text{Var}(\hat{M}) = \Theta\left(\frac{D}{N_U N_M^{k+1}}\right), \quad (21)$$

$$\text{Var}(\hat{M}_L) = O\left(\frac{D^{\log_2 3}}{N_U N_M^{k+1}}\right),$$

where \hat{M} and \hat{M}_L are constructed with the measurement data from the protocols in Algorithm 1 and Algorithm 2, respectively.

For the global random unitary case, we rigorously prove that the variance scales linearly with D , N_U^{-1} , and $N_M^{-(k+1)}$; while for the local random unitary case, we provide an upper bound on the scaling. No matter in the global or the local case, such error scaling is much better than full tomography [56]. In addition, the variance decreases when increasing the party number k , which is equivalent to the number of virtual copies of state. In Appendices E and F, we provide a detailed analysis of the statistical variance.

To support our theoretical analysis, we conduct numerical experiments for the local protocol, i.e., the random unitary matrix applied is the tensor product of the

random qubit ones. The numerical results are shown in Fig. 4. In Fig. 4(a)-4(c), we choose the tripartite Greenberger-Horne-Zeilinger (GHZ) state, with an equal qubit number in each party, as the target state. The exact value $T_3 = 0.125$ is independent of the qubit number, so that the variance itself is suitable to quantify the quality of the estimation result. We first show how the variance changes with N_U when measuring a three-qubit GHZ state for different N_M in Fig. 4(a). These three lines with slopes about -1 are coincident with the conclusion in Proposition 3 that $\text{Var}(\hat{M}_L) \propto N_U^{-1}$. The variance decreases with the increase of N_M , the measurement times per unitary evolution. Then, by adjusting the qubit number of the GHZ state and with a fixed $N_M = 10$, we also find that the variance increases for larger system dimension in Fig. 4(b).

To study how the variance scales with dimension D when $D \gg N_M$, we change the qubit number of the target GHZ state from 6 to 21 and set $N_U = 100$ and $N_M = 10$ in Fig. 4(c). The slope $\alpha = 1.2587$ from the linear regression of $\log_2 [\text{Var}(\hat{M}_L)]$ and the qubit number n . It indicates $\text{Var}(\hat{M}_L) \propto D^\alpha$ with $\alpha \approx 1.26 < \log_2 3$, which is consistent with our theoretical result in Proposition 3. In Fig. 4(d), we take a six-qubit noisy W state as an example, show the measurement results for different N_M with $N_U = 100$, and find that our protocol can provide such high-quality measurement results as $N_M \geq 20$.

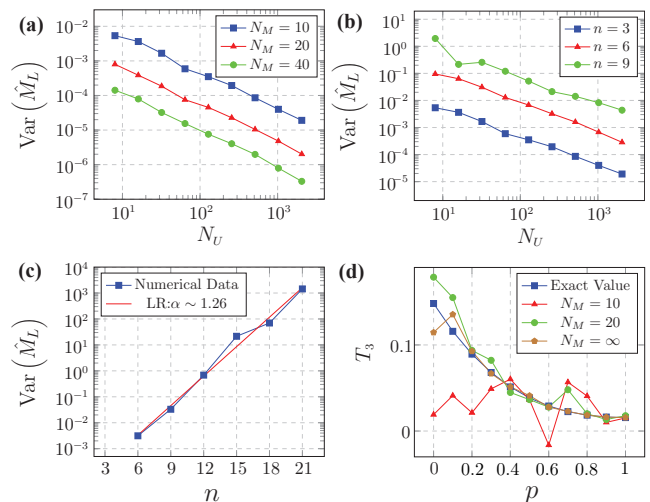


FIG. 4. Numerical results for the estimation of the tripartite CRO T_3 in Eq. (5) with the local measurement protocol. (a) The variance scaling with N_U for different N_M when measuring the three-qubit GHZ state. (b) The variance scaling with N_U when measuring the GHZ state with different number of qubits, and $N_M = 10$. (c) The variance dependence on the number of qubits of the measured GHZ state with $N_U = 100$ and $N_M = 10$. We linearly regress the data and obtain the slope $\alpha = 1.2587$. (d) The estimation for the noisy state. We measure T_3 of a six-qubit noisy W state $\rho_{ABC} = (1-p)|W\rangle\langle W| + \frac{p}{2^6}I$ with $N_U = 100$ and different N_M .

V. APPLICATION TO MEASURING FIDELITY TO MAXIMALLY ENTANGLED STATES

Our protocol can also be modified to measure the fidelity between the candidate bipartite state, and that of a maximally entangled state,

$$|\Psi^+\rangle = \frac{1}{\sqrt{d}} \sum_{i=1}^d |ii\rangle, \quad (22)$$

on $\mathcal{H}_A \otimes \mathcal{H}_B$. This fidelity is important in entanglement detection [18] and many quantum communication tasks [2]. Prior methods need an ideally prepared state [45] or fixed basis measurements. Utilizing random measurements, the maximally entangled state can be virtually produced by postprocessing, and randomness may make it more robust against the noise in the measurement basis.

Without loss of generality, we consider $d = 2^n$ with n being the qubit number of each party. Recall that the outer product form of the SWAP operator is $S = \sum_{i,j=1}^d |i\rangle\langle j| \otimes |j\rangle\langle i|$, and the maximally entangled state is proportional to the partial transpose of S as follows.

$$\begin{aligned} |\Psi^+\rangle\langle\Psi^+| &= \frac{1}{d} \sum_{i,j=1}^d |i\rangle\langle j| \otimes |i\rangle\langle j| \\ &= \frac{1}{d} \left(\sum_{i,j=1}^d |i\rangle\langle j| \otimes |j\rangle\langle i| \right)^{T_B} = \frac{1}{d} S^{T_B}, \end{aligned} \quad (23)$$

and the corresponding diagrams are shown in Figs. 5(a) and 5(b).

Suppose the state we actually produce is $\rho \in \mathcal{H}_A \otimes \mathcal{H}_B$. According to Eq. (23), the fidelity between ρ and $|\Psi^+\rangle$ can be represented using S as

$$\text{tr}(\rho|\Psi^+\rangle\langle\Psi^+|) = \frac{1}{d} \text{tr}(\rho S^{T_B}). \quad (24)$$

Recall that Eq. (10) shows that the SWAP operator can be effectively generated by randomized measurements. Hence the fidelity can be further rewritten as

$$\begin{aligned} \text{tr}(\rho|\Psi^+\rangle\langle\Psi^+|) &= \frac{1}{d} \text{tr}(\rho[\Phi^2(X)]^{T_B}) \\ &= \frac{1}{d} \text{tr} \left\{ \rho \mathbb{E}_U [(U \otimes U)^\dagger X (U \otimes U)]^{T_B} \right\} \\ &= \frac{1}{d} \text{tr} \left\{ \mathbb{E}_U [(U \otimes U^*) \rho (U^\dagger \otimes U^T)] X \right\}. \end{aligned} \quad (25)$$

In the final equality, we use the fact that X is a diagonal matrix such that $X^{T_B} = X$, and also the cyclic property of trace to put the unitary evolution on the state (see Fig. 5 for an illustration).

Similar as for the local unitary protocol shown in Sec. III, one can apply the local random unitary $U =$

$\otimes_{i=1}^n U_i$ here. As a result, the postprocessing matrix is substituted by $\tilde{X}(\vec{s}_A, \vec{s}_B) = \prod_i X_i(s_i^A, s_i^B) = 2^n (-2)^{-D[\vec{s}_A, \vec{s}_B]}$ as in Eq. (13). Note that here the postprocessing function is on the measurement result of the two parties A and B , not on the different copies as before. We summarize the postprocessing under local random unitary as follows.

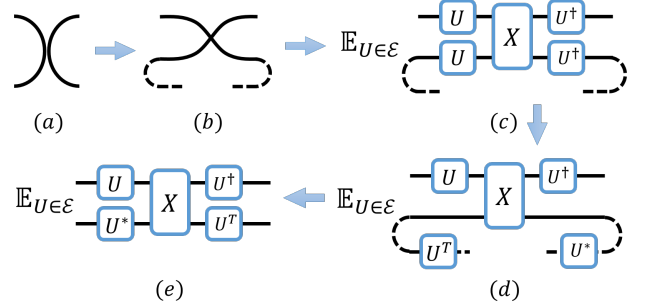


FIG. 5. Diagrammatic illustration of the derivation in Eq. (25). $\mathbb{E}_{U \in \mathcal{E}}$ denotes averaging over (qubit) unitary 2-design and the dotted lines represent the transposition on the second subsystem. (a) $d|\Psi^+\rangle\langle\Psi^+| \rightarrow$ (b) $S^{T_B} \rightarrow$ (c) $[\Phi^2(X)]^{T_B} = \mathbb{E}_U [(U \otimes U)X(U \otimes U)^\dagger]^{T_B} \rightarrow$ (d) $\mathbb{E}_U [(U \otimes U^*)X^{T_B}(U^\dagger \otimes U^T)] \rightarrow$ (e) $\mathbb{E}_U [(U \otimes U^*)X(U^\dagger \otimes U^T)]$.

Proposition 4. For a bipartite state ρ_{AB} with subsystems A and B both containing n qubits, the fidelity of a state ρ_{AB} with the maximally entangled state $|\Psi^+\rangle$ can be expressed by the following local randomized measurement result:

$$\begin{aligned} \text{tr}(\rho_{AB}|\Psi^+\rangle\langle\Psi^+|) &= \sum_{\vec{s}_A, \vec{s}_B} (-2)^{-D[\vec{s}_A, \vec{s}_B]} \mathbb{E}_U \text{Pr}(\vec{s}_A, \vec{s}_B|U), \\ \text{Pr}(\vec{s}_A, \vec{s}_B|U) &= \text{tr}[(U \otimes U^*)\rho(U^\dagger \otimes U^T)|\vec{s}_A, \vec{s}_B\rangle\langle\vec{s}_A, \vec{s}_B|], \end{aligned} \quad (26)$$

where $P(\vec{s}_A, \vec{s}_B|U)$ is the probability when measuring $(U \otimes U^*)\rho(U^\dagger \otimes U^T)$ in the computational basis $\{|\vec{s}_A, \vec{s}_B\rangle\}$; the random unitary $U = \otimes_{i=1}^n U_i$ is a tensor product of unitaries on each qubit, where each U_i is sampled from a unitary 2-design.

Based on Proposition 4, we summarize the fidelity measurement protocol in Algorithm 3.

Algorithm 3 Fidelity with Local Measurement

Input: $N_U \times N_M$ sequentially prepared ρ_{AB} with subsystems A and B both containing n qubits.

Output: Probabilities measured in computational measurement basis under random unitary evolution $\Pr(\vec{s}_A, \vec{s}_B|U)$.

```

1: for  $i = 1$  to  $N_U$  do
2:   Randomly pick a unitary matrix  $U = \bigotimes_{i=1}^n U_i$ , where
    $U_i$  on each qubit forms a unitary 2-design. Operate  $U \otimes U^*$ 
   on  $\rho$  to get  $(U \otimes U^*)\rho(U^\dagger \otimes U^T)$ .
3:   for  $j = 1$  to  $N_M$  do
4:     Measure  $(U \otimes U^*)\rho(U^\dagger \otimes U^T)$  in the computational
     basis  $\{|\vec{s}_A, \vec{s}_B\rangle\}$ .
5:     Record the measurement results.
6:   end for
7:   Estimate the probabilities  $\Pr(\vec{s}_A, \vec{s}_B|U)$ .
8: end for
9: Do the data postprocessing according to Proposition 4.
```

In Appendix G, we also extend the randomized measurement method to estimate the concurrence [57, 58] of an n -qubit quantum state. This shows the broad application scenarios of the randomized measurements.

VI. DISCUSSION

In this work, we introduce an operationally meaningful quantifier of the total correlation within a multipartite quantum system motivated by experimental accessibility. Based on this definition, we design a protocol to estimate the total correlation of a candidate state using only classical postprocessing of data collected from randomized single-qubit measurements, and show that the number of measurements required is significantly lower than that of the state tomography. Taken together, the results provide an accessible tool for characterizing multipartite correlations in NISQ devices.

There are a number of interesting future directions. One direction involves observing that shadow estimation offers an alternative way to postprocess the measurement data under random unitary evolution [34]. Recently, there are enhancements of the error scaling of the shadow protocol by using prior knowledge of the observable [59–

61], or the intrinsic tensor-product structure of the underlying state for the nonlinear function estimation [51]. It would be interesting to ascertain if these methodologies could provide further enhancement to estimating the total correlation measurement here, in situations where one has additional knowledge of the NISQ device [62].

The total correlation has many proposed applications. A recent framework for characterizing fine-grained structure or genuine multipartite correlation, for example, involves measuring how correlation changes depending on how one partitions the whole system [10, 12]. Meanwhile, such correlation measure could be used as the cost function in the near-term variational algorithms to decouple the quantum system [63–66]. Both scenarios would require many costly repeated calls to estimate the correlation. Thus, a natural direction then is to investigate if our techniques provide the reduction to this cost. Meanwhile, many occasions invoke interest in specific types of correlations, such as those that are classical, or purely quantum mechanical, which is also interesting to further investigate with randomized measurements.

VII. ACKNOWLEDGMENTS

We thank Arthur Jaffe and Xiongfeng Ma for the useful discussion. This research is supported by the Quantum Engineering Program QEP-SF3, National Research Foundation of Singapore under its NRF-ANR joint program (NRF2017-NRF-ANR004 VanQuTe), the Singapore Ministry of Education Tier 1 grant RG162/19, FQXi-RFP-IPW-1903 from the foundational Questions Institute and Fetzer Franklin Fund, a donor advised fund of Silicon Valley Community Foundation, the National Natural Science Foundation of China Grants No. 11875173 and No. 1217040781, and the National Key Research and Development Program of China Grants No. 2019QY0702 and No. 2017YFA0303903. Any opinions, findings and conclusions or recommendations expressed in this material are those of the author(s) and do not reflect the views of the National Research Foundation, Singapore.

-
- [1] J. Preskill, Quantum Computing in the NISQ era and beyond, *Quantum* **2**, 79 (2018).
 - [2] R. Horodecki, P. Horodecki, M. Horodecki, and K. Horodecki, Quantum entanglement, *Rev. Mod. Phys.* **81**, 865 (2009).
 - [3] K. Modi, A. Brodutch, H. Cable, T. Paterek, and V. Vedral, The classical-quantum boundary for correlations: Discord and related measures, *Rev. Mod. Phys.* **84**, 1655 (2012).
 - [4] J. Eisert, D. Hangleiter, N. Walk, I. Roth, D. Markham, R. Parekh, U. Chabaud, and E. Kashefi, Quantum certification and benchmarking, *Nature Reviews Physics* **2**, 382 (2020).
 - [5] M. Kliesch and I. Roth, Theory of quantum system certification, *PRX Quantum* **2**, 010201 (2021).
 - [6] K. Modi, T. Paterek, W. Son, V. Vedral, and M. Williamson, Unified view of quantum and classical correlations, *Phys. Rev. Lett.* **104**, 080501 (2010).
 - [7] J. Goold, M. Huber, A. Riera, L. del Rio, and P. Skrzypczyk, The role of quantum information in thermodynamics—a topical review, *Journal of Physics A: Mathematical and Theoretical* **49**, 143001 (2016).
 - [8] G. D. Chiara and A. Sanpera, Genuine quantum correlations in quantum many-body systems: a review of recent progress, *Reports on Progress in Physics* **81**, 074002 (2018).

- [9] J. Goold, C. Gogolin, S. R. Clark, J. Eisert, A. Scardicchio, and A. Silva, Total correlations of the diagonal ensemble herald the many-body localization transition, *Phys. Rev. B* **92**, 180202 (2015).
- [10] C. H. Bennett, A. Grudka, M. Horodecki, P. Horodecki, and R. Horodecki, Postulates for measures of genuine multipartite correlations, *Phys. Rev. A* **83**, 012312 (2011).
- [11] G. L. Giorgi, B. Bellomo, F. Galve, and R. Zambrini, Genuine quantum and classical correlations in multipartite systems, *Phys. Rev. Lett.* **107**, 190501 (2011).
- [12] D. Girolami, T. Tufarelli, and C. E. Susa, Quantifying genuine multipartite correlations and their pattern complexity, *Phys. Rev. Lett.* **119**, 140505 (2017).
- [13] S. Mandal, M. Narozniak, C. Radhakrishnan, Z.-Q. Jiao, X.-M. Jin, and T. Byrnes, Characterizing coherence with quantum observables, *Phys. Rev. Research* **2**, 013157 (2020).
- [14] R. Islam, R. Ma, P. M. Preiss, M. Eric Tai, A. Lukin, M. Rispoli, and M. Greiner, Measuring entanglement entropy in a quantum many-body system, *Nature* **528**, 77 (2015).
- [15] A. M. Kaufman, M. E. Tai, A. Lukin, M. Rispoli, R. Schittko, P. M. Preiss, and M. Greiner, Quantum thermalization through entanglement in an isolated many-body system, *Science* **353**, 794 (2016).
- [16] T. Brydges, A. Elben, P. Jurcevic, B. Vermersch, C. Maier, B. P. Lanyon, P. Zoller, R. Blatt, and C. F. Roos, Probing rényi entanglement entropy via randomized measurements, *Science* **364**, 260 (2019).
- [17] N. Linden, M. Mosonyi, and A. Winter, The structure of rényi entropic inequalities, *Proceedings of the Royal Society A: Mathematical, Physical and Engineering Sciences* **469**, 20120737 (2013).
- [18] O. Gühne and G. Toth, Entanglement detection, *Physics Reports* **474**, 1 (2009).
- [19] N. Friis, G. Vitagliano, M. Malik, and M. Huber, Entanglement certification from theory to experiment, *Nature Reviews Physics* **1**, 72 (2019).
- [20] M. Huber and J. I. de Vicente, Structure of multidimensional entanglement in multipartite systems, *Phys. Rev. Lett.* **110**, 030501 (2013).
- [21] F. Shahandeh, J. Sperling, and W. Vogel, Structural quantification of entanglement, *Phys. Rev. Lett.* **113**, 260502 (2014).
- [22] H. Lu, Q. Zhao, Z.-D. Li, X.-F. Yin, X. Yuan, J.-C. Hung, L.-K. Chen, L. Li, N.-L. Liu, C.-Z. Peng, Y.-C. Liang, X. Ma, Y.-A. Chen, and J.-W. Pan, Entanglement structure: Entanglement partitioning in multipartite systems and its experimental detection using optimizable witnesses, *Phys. Rev. X* **8**, 021072 (2018).
- [23] Y. Zhou, Q. Zhao, X. Yuan, and X. Ma, Detecting multipartite entanglement structure with minimal resources, *npj Quantum Information* **5**, 1 (2019).
- [24] G. Tóth and O. Gühne, Detecting genuine multipartite entanglement with two local measurements, *Phys. Rev. Lett.* **94**, 060501 (2005).
- [25] H. Zhu, Y. S. Teo, and B.-G. Englert, Minimal tomography with entanglement witnesses, *Phys. Rev. A* **81**, 052339 (2010).
- [26] J. Dai, Y. L. Len, Y. S. Teo, B.-G. Englert, and L. A. Krivitsky, Experimental detection of entanglement with optimal-witness families, *Phys. Rev. Lett.* **113**, 170402 (2014).
- [27] Y. Zhou, Entanglement detection under coherent noise: Greenberger-horne-zeilinger-like states, *Phys. Rev. A* **101**, 012301 (2020).
- [28] Y.-C. Liang, Y.-H. Yeh, P. E. M. F. Mendonça, R. Y. Teh, M. D. Reid, and P. D. Drummond, Quantum fidelity measures for mixed states, *Reports on Progress in Physics* **82**, 076001 (2019).
- [29] A. K. Ekert, C. M. Alves, D. K. L. Oi, M. Horodecki, P. Horodecki, and L. C. Kwék, Direct estimations of linear and nonlinear functionals of a quantum state, *Phys. Rev. Lett.* **88**, 217901 (2002).
- [30] S. J. van Enk and C. W. J. Beenakker, Measuring $\text{Tr}\rho^n$ on single copies of ρ using random measurements, *Phys. Rev. Lett.* **108**, 110503 (2012).
- [31] A. Elben, B. Vermersch, M. Dalmonte, J. I. Cirac, and P. Zoller, Rényi entropies from random quenches in atomic hubbard and spin models, *Phys. Rev. Lett.* **120**, 050406 (2018).
- [32] P. J. Coles, M. Cerezo, and L. Cincio, Strong bound between trace distance and hilbert-schmidt distance for low-rank states, *Phys. Rev. A* **100**, 022103 (2019).
- [33] N. Yu, Quantum closeness testing: A streaming algorithm and applications, [arXiv:1904.03218](https://arxiv.org/abs/1904.03218) (2019).
- [34] H.-Y. Huang, R. Kueng, and J. Preskill, Predicting many properties of a quantum system from very few measurements, *Nature Physics* **16**, 1050 (2020).
- [35] A. Elben, R. Kueng, H.-Y. R. Huang, R. van Bijnen, C. Kokail, M. Dalmonte, P. Calabrese, B. Kraus, J. Preskill, P. Zoller, and B. Vermersch, Mixed-state entanglement from local randomized measurements, *Phys. Rev. Lett.* **125**, 200501 (2020).
- [36] Y. Zhou, P. Zeng, and Z. Liu, Single-copies estimation of entanglement negativity, *Phys. Rev. Lett.* **125**, 200502 (2020).
- [37] A. Neven, J. Carrasco, V. Vitale, C. Kokail, A. Elben, M. Dalmonte, P. Calabrese, P. Zoller, B. Vermersch, R. Kueng, and B. Kraus, Symmetry-resolved entanglement detection using partial transpose moments, *npj Quantum Information* **7**, 152 (2021).
- [38] M. C. Tran, B. Dakić, W. Laskowski, and T. Paterek, Correlations between outcomes of random measurements, *Phys. Rev. A* **94**, 042302 (2016).
- [39] A. Ketterer, N. Wyderka, and O. Gühne, Characterizing multipartite entanglement with moments of random correlations, *Phys. Rev. Lett.* **122**, 120505 (2019).
- [40] L. Knips, J. Dziewior, W. Kobus, W. Laskowski, T. Paterek, P. J. Shadbolt, H. Weinfurter, and J. D. A. Meinicke, Multipartite entanglement analysis from random correlations, *npj Quantum Information* **6**, 51 (2020).
- [41] A. Ketterer, N. Wyderka, and O. Gühne, Entanglement characterization using quantum designs, *Quantum* **4**, 325 (2020).
- [42] A. Ketterer, S. Imai, N. Wyderka, and O. Gühne, Statistically significant tests of multiparticle quantum correlations based on randomized measurements, [arXiv:2012.12176 \[quant-ph\]](https://arxiv.org/abs/2012.12176) (2021).
- [43] A. Rath, C. Branciard, A. Minguzzi, and B. Vermersch, Quantum fisher information from randomized measurements, *Phys. Rev. Lett.* **127**, 260501 (2021).
- [44] M. Yu, D. Li, J. Wang, Y. Chu, P. Yang, M. Gong, N. Goldman, and J. Cai, Experimental estimation of the quantum fisher information from randomized measurements, [arXiv:2104.00519](https://arxiv.org/abs/2104.00519) (2021).

- [45] A. Elben, B. Vermersch, R. van Bijnen, C. Kokail, T. Brydges, C. Maier, M. K. Joshi, R. Blatt, C. F. Roos, and P. Zoller, Cross-platform verification of intermediate scale quantum devices, *Phys. Rev. Lett.* **124**, 010504 (2020).
- [46] W.-H. Zhang, C. Zhang, Z. Chen, X.-X. Peng, X.-Y. Xu, P. Yin, S. Yu, X.-J. Ye, Y.-J. Han, J.-S. Xu, G. Chen, C.-F. Li, and G.-C. Guo, Experimental optimal verification of entangled states using local measurements, *Phys. Rev. Lett.* **125**, 030506 (2020).
- [47] T. Zhang, J. Sun, X.-X. Fang, X.-M. Zhang, X. Yuan, and H. Lu, Experimental quantum state measurement with classical shadows, *Phys. Rev. Lett.* **127**, 200501 (2021).
- [48] B. Vermersch, A. Elben, L. M. Sieberer, N. Y. Yao, and P. Zoller, Probing scrambling using statistical correlations between randomized measurements, *Phys. Rev. X* **9**, 021061 (2019).
- [49] A. Elben, J. Yu, G. Zhu, M. Hafezi, F. Pollmann, P. Zoller, and B. Vermersch, Many-body topological invariants from randomized measurements in synthetic quantum matter, *Science Advances* **6**, eaaz3666 (2020).
- [50] Z.-P. Cian, H. Deghani, A. Elben, B. Vermersch, G. Zhu, M. Barkeshli, P. Zoller, and M. Hafezi, Many-body chern number from statistical correlations of randomized measurements, *Phys. Rev. Lett.* **126**, 050501 (2021).
- [51] R. J. Garcia, Y. Zhou, and A. Jaffe, Quantum scrambling with classical shadows, *Phys. Rev. Research* **3**, 033155 (2021).
- [52] A. Elben, B. Vermersch, C. F. Roos, and P. Zoller, Statistical correlations between locally randomized measurements: A toolbox for probing entanglement in many-body quantum states, *Phys. Rev. A* **99**, 052323 (2019).
- [53] D. P. DiVincenzo, D. W. Leung, and B. M. Terhal, Quantum data hiding, *IEEE Transactions on Information Theory* **48**, 580 (2002).
- [54] C. Dankert, R. Cleve, J. Emerson, and E. Livine, Exact and approximate unitary 2-designs and their application to fidelity estimation, *Phys. Rev. A* **80**, 012304 (2009).
- [55] H. Zhu, R. Kueng, M. Grassl, and D. Gross, The clifford group fails gracefully to be a unitary 4-design, [arXiv:1609.08172](https://arxiv.org/abs/1609.08172) (2016).
- [56] J. Haah, A. W. Harrow, Z. Ji, X. Wu, and N. Yu, Sample-optimal tomography of quantum states, *IEEE Transactions on Information Theory* **63**, 5628 (2017).
- [57] W. K. Wootters, Entanglement of formation and concurrence, *Quantum Inf. Comput.* **1**, 27 (2001).
- [58] J. F. Beacom and M. R. Vagins, Antineutrino spectroscopy with large water Čerenkov detectors, *Phys. Rev. Lett.* **93**, 171101 (2004).
- [59] C. Hadfield, S. Bravyi, R. Raymond, and A. Mezzacapo, Measurements of quantum hamiltonians with locally-biased classical shadows, [arXiv:2006.15788](https://arxiv.org/abs/2006.15788) (2020).
- [60] H.-Y. Huang, R. Kueng, and J. Preskill, Efficient estimation of pauli observables by derandomization, [arXiv:2103.07510](https://arxiv.org/abs/2103.07510) (2021).
- [61] B. Wu, J. Sun, Q. Huang, and X. Yuan, Overlapped grouping measurement: A unified framework for measuring quantum states, [arXiv:2105.13091](https://arxiv.org/abs/2105.13091) (2021).
- [62] A. Rath, R. van Bijnen, A. Elben, P. Zoller, and B. Vermersch, Importance sampling of randomized measurements for probing entanglement, *Phys. Rev. Lett.* **127**, 200503 (2021).
- [63] X. Yuan, S. Endo, Q. Zhao, Y. Li, and S. C. Benjamin, Theory of variational quantum simulation, *Quantum* **3**, 191 (2019).
- [64] M. Cerezo, A. Arrasmith, R. Babbush, S. C. Benjamin, S. Endo, K. Fujii, J. R. McClean, K. Mitarai, X. Yuan, L. Cincio, *et al.*, Variational quantum algorithms, [arXiv:2012.09265](https://arxiv.org/abs/2012.09265) (2020).
- [65] S. Khatri, R. LaRose, A. Poremba, L. Cincio, A. T. Sornborger, and P. J. Coles, Quantum-assisted quantum compiling, *Quantum* **3**, 140 (2019).
- [66] Z.-J. Zhang, T. H. Kyaw, J. Kottmann, M. Degroote, and A. Aspuru-Guzik, Mutual information-assisted adaptive variational quantum eigensolver, *Quantum Science and Technology* (2021).
- [67] K. Zyczkowski and M. Kus, Random unitary matrices, *Journal of Physics A: Mathematical and General* **27**, 4235 (1994).
- [68] R. Goodman and N. R. Wallach, *Representations and invariants of the classical groups* (Cambridge University Press, 2000).
- [69] Y. Gu, *Moments of random matrices and weingarten functions*, *Ph.D. thesis* (2013).
- [70] C. C. Lindner and C. A. Rodger, *Design theory* (CRC press, 2017).
- [71] C. J. Wood, J. D. Biamonte, and D. G. Cory, Tensor networks and graphical calculus for open quantum systems, *Quantum Information & Computation* **15**, 759 (2015).
- [72] H. Shapourian, S. Liu, J. Kudler-Flam, and A. Vishwanath, Entanglement negativity spectrum of random mixed states: A diagrammatic approach, *PRX Quantum* **2**, 030347 (2021).
- [73] C.-J. Zhang, Y.-S. Zhang, S. Zhang, and G.-C. Guo, Entanglement detection beyond the computable cross-norm or realignment criterion, *Phys. Rev. A* **77**, 060301 (2008).
- [74] C. Kai and L. A. Wu, A matrix realignment method for recognizing entanglement, *Quantum Information and Computation* **3**, 193 (2002).
- [75] J. I. de Vicente, Further results on entanglement detection and quantification from the correlation matrix criterion, *Journal of Physics A: Mathematical and Theoretical* **41**, 065309 (2008).
- [76] L. Aolita and F. Mintert, Measuring multipartite concurrence with a single factorizable observable, *Phys. Rev. Lett.* **97**, 050501 (2006).

Appendix A: Preliminaries

1. Integral of random unitary matrix

A random unitary matrix is a random variable in the space of a unitary matrix [67]; Haar measure means that the probability distribution is uniform. Based on the definition of Haar-measured random unitary matrix, here we introduce a t -fold twirling channel,

$$\Phi^t(O) = \int_{\text{Haar}} dU U^{\otimes t} O U^{\dagger \otimes t}, \quad (\text{A1})$$

where $U \in \mathcal{H}_d$ and O is a linear operator acting on $\mathcal{H}_d^{\otimes t}$. According to Schur-Weyl duality [5, 68], such twirling channel is equivalent to the operation that projects O into the symmetric subspace. So we have

$$\Phi^t(O) = \int_{\text{Haar}} dU U^{\otimes t} O U^{\dagger \otimes t} = \sum_{\pi, \sigma \in \mathcal{S}_t} C_{\pi, \sigma} \text{tr}(W_\pi O) W_\sigma. \quad (\text{A2})$$

Where \mathcal{S}_t is the t -th order permutation group, $C_{\pi, \sigma}$ is the element of the Weingarten matrix [69], and W_π is the permutation operator corresponding to π . By adjusting O , one can generate any permutation operators; this is the core idea of the estimation protocol proposed in Sec. III.

Generally speaking, it is impractical to randomly pick an element in unitary space. Fortunately, it has been proved that a t -fold twirling channel can be realized by averaging over a unitary ensemble \mathcal{E} within which the elements are all fixed unitary matrices, which we call \mathcal{E} unitary t -design [70].

$$\Phi_{\mathcal{E}}^t(O) = \frac{1}{|\mathcal{E}|} \sum_{U \in \mathcal{E}} U^{\otimes t} O U^{\dagger \otimes t} = \mathbb{E}_{U \in \mathcal{E}} (U^{\otimes t} O U^{\dagger \otimes t}) = \Phi^t(O), \quad (\text{A3})$$

where $|\mathcal{E}|$ denotes the size of \mathcal{E} . This fact further reduces the difficulty of implementing twirling channel in real experiments. It is worth mentioning that the Clifford group is a unitary 3-design and a unitary t -design is also an unitary m -design with $m < t$.

2. Tensor network basics

Tensor network is one of the graphical methods helping us to deal with tensor calculation [71, 72]. In tensor networks, a tensor is represented as a box with open legs, which are indices of this tensor. For example, $\rho_{ABC} = \sum_{i,j,k,i',j',k'} \rho_{ijk,i'j'k'} |ijk\rangle \langle i'j'k'|$ is represented as a box with six legs, three of which are left, representing row indices i, j, k , and the other three are right, representing column indices i', j', k' . Open legs represent the noncontracting indices, so the connection of legs is the contraction of indices. For example, tensor AB is graphically represented by connecting the right legs of box A and the left legs of box B . $\text{tr}(A) = \sum_i A_{i,i}$ is the contraction of the row and column index of A , which can be represented by connecting the left and right legs of box A . In addition, tensor product is the operation that does not contract indices. So, to represent $A \otimes B$, we just put boxes A and B together.

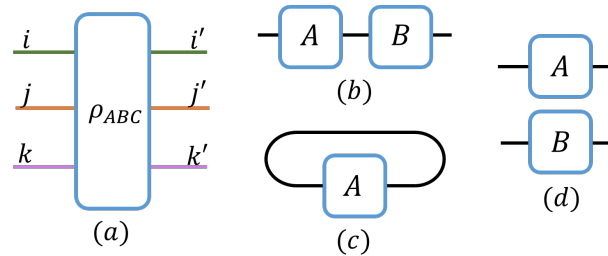


FIG. 6. (a) $\rho_{ABC} = \sum_{i,j,k,i',j',k'} \rho_{ijk,i'j'k'} |ijk\rangle \langle i'j'k'|$. (b) AB . (c) $\text{tr}(A)$. (d) $A \otimes B$

The unnormalized maximally entangled state (UMES) and SWAP operator are two commonly used operators. UMES $\sqrt{d}|\Psi^+\rangle = \sum_{i=1}^d |ii\rangle$ is represented as a semicircle with both ends to the left, where d is the dimension of Hilbert

space. Many operations can be represented using UMES. Take $A = \sum_{i,j} A_{i,j} |i\rangle\langle j|$ as an example:

$$d\langle\Psi^+|A|\Psi^+\rangle = \sum_k \langle kk| \sum_{i,j} A_{i,j} |i\rangle\langle j| \sum_l |ll\rangle = \sum_{i,j} A_{i,j} \sum_{k,l} \langle k|i\rangle\langle j|l\rangle\langle k|l\rangle = \sum_{i,j} A_{i,j} |j\rangle\langle i| = A^T \quad (\text{A4})$$

and

$$d\langle\Psi^+|A \otimes I|\Psi^+\rangle = \sum_k \langle kk| \sum_{i,j} A_{i,j} |i\rangle\langle j| \otimes I \sum_l |ll\rangle = \sum_{i,j} A_{i,j} \sum_{k,l} \langle k|i\rangle\langle j|l\rangle\langle k|l\rangle = \sum_i A_{i,i} = \text{tr}(A). \quad (\text{A5})$$

$\text{tr}(A)$ has been shown in Fig. 6(c). SWAP S , exchanging two indices, can be graphically represented with two crossed curved lines. Using this representation, one can easily prove that $\text{tr}[S(A \otimes B)] = \text{tr}(AB)$, as shown in Fig. 7.

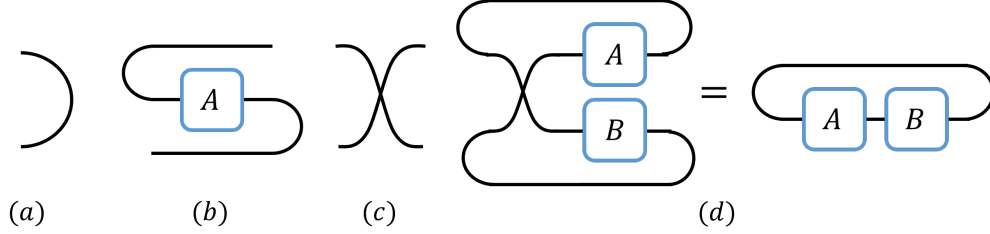


FIG. 7. (a) $\sqrt{d}|\Psi^+\rangle = \sum_{i=1} |ii\rangle$. (b) A^T . (c) S . (d) $\text{tr}[S(A \otimes B)] = \text{tr}(AB)$.

Appendix B: The property of total correlation measure defined in Eq. (1)

Recall that we take $C(\rho) = -\log_2 \mathcal{F}(\rho, \bigotimes_{i=1}^k \rho_i)$, and the fidelity measure could be

$$\mathcal{F}_{\max}(\rho, \sigma) = \frac{\text{tr}(\rho\sigma)}{\max\{\text{tr}(\rho^2), \text{tr}(\sigma^2)\}} \quad (\text{B1})$$

and

$$\mathcal{F}_{\text{GM}}(\rho, \sigma) = \frac{\text{tr}(\rho\sigma)}{\sqrt{\text{tr}(\rho^2) \text{tr}(\sigma^2)}}, \quad (\text{B2})$$

which is the one used in the main text. Note that the difference is that the denominator is either maximization or geometric mean of the purity, and one can also choose other fidelity measures [28]. We take $C(\rho) = -\log_2 \mathcal{F}_{\text{GM}}(\rho, \bigotimes_{i=1}^k \rho_i)$ as an example to discuss its property. The discussion of $C(\rho) = -\log_2 \mathcal{F}_{\max}(\rho, \bigotimes_{i=1}^k \rho_i)$ is quite similar.

- (1) $C(\rho)$ is a faithful total correlation measure, $C(\rho) = 0$ iff $\rho = \bigotimes_{i=1}^k \rho_i$, and non-negative for any ρ . This property directly follows from the property of fidelity: $\mathcal{F}_{\text{GM}}(\rho, \sigma) < 1$, $\forall \rho, \sigma$ and $\mathcal{F}_{\text{GM}}(\rho, \sigma) = 1$ iff $\rho = \sigma$.
- (2) Adding a new party ρ_{k+1} to a k -partite state ρ will not cause the increase of the total correlation in the resulting $(k+1)$ -partite tensor state $\rho \otimes \rho_{k+1}$, i.e. $C(\rho \otimes \rho_{k+1}) = C(\rho)$.

Proof.

$$\begin{aligned} \mathcal{F}_{\text{GM}}(\rho \otimes \rho_{k+1}, \bigotimes_{i=1}^k \rho_i \otimes \rho_{k+1}) &= \frac{\text{tr}[(\rho \otimes \rho_{k+1})(\bigotimes_{i=1}^k \rho_i \otimes \rho_{k+1})]}{\sqrt{\text{tr}[(\rho \otimes \rho_{k+1})^2] \text{tr}[(\bigotimes_{i=1}^k \rho_i \otimes \rho_{k+1})^2]}} \\ &= \frac{\text{tr}(\rho \bigotimes_{i=1}^k \rho_i) \text{tr} \rho_{k+1}^2}{\sqrt{\text{tr} \rho^2 \prod_{i=1}^k \text{tr} \rho_i^2} \text{tr} \rho_{k+1}^2} \\ &= \mathcal{F}_{\text{GM}}(\rho, \bigotimes_{i=1}^k \rho_i). \end{aligned} \quad (\text{B3})$$

Hence

$$C(\rho \otimes \rho_{k+1}) = -\log_2 \mathcal{F}_{\text{GM}}(\rho \otimes \rho_{k+1}, \bigotimes_{i=1}^k \rho_i \otimes \rho_{k+1}) = -\log_2 \mathcal{F}_{\text{GM}}(\rho, \bigotimes_{i=1}^k \rho_i) = C(\rho). \quad (\text{B4})$$

□

(3) $C(\rho)$ is not changed under local unitary transformation, i.e. $C(\bigotimes_{i=1}^k u_i \rho \bigotimes_{i=1}^k u_i^\dagger) = C(\rho)$.

(4) Local quantum channel, i.e., $\bigotimes_{i=1}^k \Lambda_i$, cannot create total correlation in uncorrelated k -partite state $\rho = \bigotimes_{i=1}^k \rho_i$.

Proof. Acting the local channel on the uncorrelated state, the resulting state is still uncorrelated:

$$\bigotimes_{i=1}^k \Lambda_i \left(\bigotimes_{i=1}^k \rho_i \right) = \bigotimes_{i=1}^k \Lambda_i(\rho_i). \quad (\text{B5})$$

Therefore, the faithfulness of $\mathcal{F}_{\text{GM}}(\cdot)$ directly leads to the invariance of total correlation:

$$C \left[\bigotimes_{i=1}^k \Lambda_i \left(\bigotimes_{i=1}^k \rho_i \right) \right] = C \left(\bigotimes_{i=1}^k \Lambda_i(\rho_i) \right) = C \left(\bigotimes_{i=1}^k \rho_i \right) = 0. \quad (\text{B6})$$

□

(5) $C(\rho)$ is additive under the tensor product. The $(k+l)$ -partite total correlation $C(\rho \otimes \sigma)$ equals the sum over of the k -partite total correlation $C(\rho)$ and l -partite total correlation $C(\sigma)$.

Proof.

$$\begin{aligned} \mathcal{F}_{\text{GM}}(\rho \otimes \sigma, \bigotimes_{i=1}^k \rho_i \otimes \bigotimes_{i=1}^l \sigma_i) &= \frac{\text{tr} \left[(\rho \otimes \sigma) (\bigotimes_{i=1}^k \rho_i \otimes \bigotimes_{i=1}^l \sigma_i) \right]}{\sqrt{\text{tr} [(\rho \otimes \sigma)^2] \text{tr} \left[(\bigotimes_{i=1}^k \rho_i \otimes \bigotimes_{i=1}^l \sigma_i)^2 \right]}} \\ &= \frac{\text{tr} \left(\rho \bigotimes_{i=1}^k \rho_i \right)}{\sqrt{\text{tr} \rho^2 \prod_{i=1}^k \text{tr} \rho_i^2}} \frac{\text{tr} \left(\sigma \bigotimes_{i=1}^l \sigma_i \right)}{\sqrt{\text{tr} \sigma^2 \prod_{i=1}^l \text{tr} \sigma_i^2}} \\ &= \mathcal{F}_{\text{GM}}(\rho, \bigotimes_{i=1}^k \rho_i) \mathcal{F}_{\text{GM}}(\sigma, \bigotimes_{i=1}^l \sigma_i). \end{aligned} \quad (\text{B7})$$

Hence,

$$\begin{aligned} C(\rho \otimes \sigma) &= -\log_2 \mathcal{F}_{\text{GM}}(\rho \otimes \sigma, \bigotimes_{i=1}^k \rho_i \otimes \bigotimes_{i=1}^l \sigma_i) \\ &= -\log_2 \mathcal{F}_{\text{GM}} \left(\rho, \bigotimes_{i=1}^k \rho_i \right) - \log_2 \mathcal{F}_{\text{GM}} \left(\sigma, \bigotimes_{i=1}^l \sigma_i \right) \\ &= C(\rho) + C(\sigma). \end{aligned} \quad (\text{B8})$$

□

It is easy to prove that the other definition of total correlation, $C(\rho) = -\log_2 \mathcal{F}_{\text{max}} \left(\rho, \bigotimes_{i=1}^k \rho_i \right)$ satisfies properties (1), (2), (3) and (4), while it fails to meet the additivity condition (5).

Now we discuss how to generalize such total correlation measure to genuine multipartite correlation measure. In [10], the authors proposed three postulates that every multipartite genuine correlation measure and indicator should satisfy. They also gave a definition of multipartite genuine correlation based on those postulates: k -partite state ρ has

genuine k -partite correlation if it is nonproduct for any bipartition. Following this definition, we define the k -partite genuine correlation measure

$$C_{\text{g.c.}}(\rho) = \min_{A \subset [k]} \{-\log \mathcal{F}(\rho, \rho_A \otimes \rho_{\bar{A}})\}, \quad (\text{B9})$$

where $\mathcal{F}(\rho, \sigma)$ can also be $\mathcal{F}_{\text{max}}(\rho, \sigma)$ or $\mathcal{F}_{\text{GM}}(\rho, \sigma)$. Because of the faithfulness of these two fidelities, $C_{\text{g.c.}}(\rho) = 0$ iff ρ is the product in some bipartition $\{A, \bar{A}\}$ of the k -partite system. Hence, $C_{\text{g.c.}}(\rho)$ satisfies those three postulates proposed in [10].

Appendix C: Bipartite entanglement criterion using T_2

In [73], the authors proposed an entanglement criterion which is strictly stronger than the well-known computable cross norm criterion [74] and dV criterion (the one based on correlation tensor of states) [75],

$$\|\mathcal{R}(\rho_{AB} - \rho_A \otimes \rho_B)\| > \sqrt{(1 - \text{tr} \rho_A^2)(1 - \text{tr} \rho_B^2)}, \quad (\text{C1})$$

where $\|\cdot\|$ denotes the trace norm, and $\mathcal{R}(\cdot)$ represents the realignment operation, $\mathcal{R}(O)_{ij,kl} = O_{ik,jl}$. However, $\|\mathcal{R}(\rho_{AB} - \rho_A \otimes \rho_B)\|$ is hard to estimate by direct measurements. Hence, based on this criterion, we further construct a new measurable entanglement criterion as follows.

Proposition 5. *For any separable state ρ_{AB} , it should satisfy*

$$\text{tr} \rho_{AB}^2 + \text{tr} \rho_A^2 + \text{tr} \rho_B^2 - 2 \text{tr}[\rho_{AB}(\rho_A \otimes \rho_B)] - 1 \leq 0, \quad (\text{C2})$$

and the violation indicates the presence of entanglement.

The proof is left to Appendix C1. We name this criterion as T_2 separability criterion. Although weaker than Eq. (C1), the T_2 criterion is equivalent to the well-known Rényi entropy criterion (i.e., $\text{tr} \rho_{AB}^2 \leq \text{tr} \rho_A^2, \text{tr} \rho_B^2$ for the separable ρ_{AB}) on pure states and Bell-diagonal states, and shows stronger detection power for some asymmetric states.

$$\rho_{AB} = (1 - p)|\Psi^+\rangle\langle\Psi^+| + p|0+\rangle\langle 0+| \quad (\text{C3})$$

is the mixture of the Bell state $|\Psi^+\rangle$ and the product state $|0+\rangle$. For such state, T_2 criterion indicates entanglement for $p < 1$, which is same as positive partial transposition (PPT) criterion, the necessary and sufficient condition for (2×2) -dimensional quantum states. However, the entropy and p_3 -PPT criterion [35] only detect entanglement as $p < 0.5$ and $p < 0.59$, respectively. A detailed comparison and discussion are left to Appendix C2. It is worth mentioning that this criterion can be generalized to non-full-separability criterion in the multipartite system [73], and we leave it for future study.

1. Proof of Proposition 5

For simplicity, denote $\mathcal{R}(\rho_{AB} - \rho_A \otimes \rho_B)$ by R , and assume the dimension of \mathcal{H}_A is less than the dimension of \mathcal{H}_B $d_A \leq d_B$. Then

$$\|R\| = \sum_{i=1}^{d_A} \lambda_i, \quad (\text{C4})$$

where $\lambda_i \geq 0$ are the singular values of R . Although $\|R\|$ is hard to directly measure, we find that

$$\text{tr}(RR^\dagger) = \sum_{i=1}^{d_A} \lambda_i^2 \quad (\text{C5})$$

can be directly measured, and the value of $\|R\|$ may be bounded by $\text{tr}(RR^\dagger)$.

Lemma 1. $\sum_{i=1}^{d_A^2} \lambda_i^2$ can be represented using the purities of ρ_A , ρ_B , and ρ_{AB} and $T_2 = \text{tr}[\rho_{AB}(\rho_A \otimes \rho_B)]$:

$$\text{tr}(RR^\dagger) = \text{tr}(\rho_{AB} - \rho_A \otimes \rho_B)^2 = \text{tr} \rho_{AB}^2 + \text{tr} \rho_A^2 \text{tr} \rho_B^2 - 2 \text{tr}[\rho_{AB}(\rho_A \otimes \rho_B)]. \quad (\text{C6})$$

Proof. For simplicity, denote $\rho_{AB} - \rho_A \otimes \rho_B$ by O_{AB} . O_{AB} is Hermitian but generally not positive. Hence, we have

$$R^\dagger = [\mathcal{R}(O_{AB})^*]^T = \mathcal{R}^T(O_{AB}^T), \quad (\text{C7})$$

so that the elements of R^\dagger are the elements of O_{AB} :

$$R_{ij,kl}^\dagger = [\mathcal{R}(O_{AB}^T)]_{kl,ij} = (O_{AB}^T)_{ki,lj} = (O_{AB})_{lj,ki}. \quad (\text{C8})$$

Now we can represent $\text{tr}(RR^\dagger)$ by the index contraction of $\rho_{AB} - \rho_A \otimes \rho_B$:

$$\begin{aligned} \text{tr}(RR^\dagger) &= \sum_{i,j,k,l} R_{ij,kl} R_{kl,ij}^\dagger = \sum_{i,j,k,l} (O_{AB})_{ik,jl} (O_{AB})_{jl,ik} \\ &= \text{tr}(O_{AB})^2 = \text{tr}(\rho_{AB} - \rho_A \otimes \rho_B)^2 = \text{tr} \rho_{AB}^2 + \text{tr} \rho_A^2 \text{tr} \rho_B^2 - 2 \text{tr}[\rho_{AB}(\rho_A \otimes \rho_B)]. \end{aligned} \quad (\text{C9})$$

□

Suppose we have measured the value of $p_2 = \sum_{i=1}^{d_A^2} \lambda_i^2 = \text{tr} \rho_{AB}^2 + \text{tr} \rho_A^2 \text{tr} \rho_B^2 - 2 \text{tr}[\rho_{AB}(\rho_A \otimes \rho_B)]$. Then it can be easily proved that

$$\sqrt{p_2} \leq \sum_{i=1}^{d_A^2} \lambda_i \leq d_A \sqrt{p_2}. \quad (\text{C10})$$

The minimum is achieved when $\lambda_1 = \sqrt{p_2}$ and $\lambda_i = 0$ for $2 \leq i \leq d_A^2$ and the maximum is achieved when $\lambda_i = \sqrt{p_2}/d_A$ for $1 \leq i \leq d_A^2$. Eq. (C1) tells us that separable ρ_{AB} satisfy $\sum_{i=1}^{d_A^2} \lambda_i^2 \leq \sqrt{(1 - \text{tr} \rho_A^2)(1 - \text{tr} \rho_B^2)}$. According to the above equation, separable ρ_{AB} satisfy

$$\sqrt{p_2} \leq \sqrt{(1 - \text{tr} \rho_A^2)(1 - \text{tr} \rho_B^2)} \rightarrow \text{tr} \rho_{AB}^2 + \text{tr} \rho_A^2 + \text{tr} \rho_B^2 - 2 \text{tr}[\rho_{AB}(\rho_A \otimes \rho_B)] - 1 \leq 0. \quad (\text{C11})$$

2. Discussion of the detection power of T_2 criterion

Here we first prove the equivalence of the T_2 criterion and the entropy criterion for pure state $|\varphi_{AB}\rangle$. As is known to all, for a pure state, the entropy criterion is a necessary and sufficient condition for separability. So we only need to prove Proposition 5 is also necessary and sufficient. Taking the Schmidt decomposition of $|\varphi_{AB}\rangle$,

$$|\varphi_{AB}\rangle = \sum_{i=1}^{d_A} \sqrt{\lambda_i} |ii\rangle, \quad (\text{C12})$$

where $0 \leq \sqrt{\lambda_i} \leq 1$ are the Schmidt co-efficients. The purities can be easily calculated as

$$\text{tr} \rho_{AB}^2 = 1, \quad \text{tr} \rho_A^2 = \text{tr} \rho_B^2 = \sum_{i=1}^{d_A} \lambda_i^2, \quad (\text{C13})$$

and

$$\begin{aligned} \text{tr}[\rho_{AB}(\rho_A \otimes \rho_B)] &= \langle \varphi_{AB} | \rho_A \otimes \rho_B | \varphi_{AB} \rangle \\ &= \sum_{k,l=1}^{d_A} \sqrt{\lambda_k \lambda_l} \langle kk | \left(\sum_{i,j=1}^{d_A} \lambda_i \lambda_j |ij\rangle \langle ij| \right) | ll \rangle \\ &= \sum_{i,j,k,l=1}^{d_A} \sqrt{\lambda_k \lambda_l} \lambda_i \lambda_j \delta_{ik} \delta_{jk} \delta_{il} \delta_{jl} \\ &= \sum_{i=1}^{d_A} \lambda_i^3. \end{aligned} \quad (\text{C14})$$

Then the T_2 criterion reduces to

$$\sum_{i=1}^{d_A} \lambda_i^2 \leq \sum_{i=1}^{d_A} \lambda_i^3, \quad (\text{C15})$$

where $\sqrt{\lambda_i}$ are the Schmidt coefficients of $|\varphi_{AB}\rangle$. The normalization and singular value decomposition requires $\sum_{i=1}^{d_A} \lambda_i = 1$ and $0 \leq \lambda_i \leq 1$. So the only solution of the above inequality is $\lambda_1 = 1$ and $\lambda_i = 0$ for $2 \leq i \leq d_A$, which means $|\varphi_{AB}\rangle = |\varphi_A\rangle|\varphi_B\rangle$.

For a Bell-diagonal state with the form

$$\rho_{AB} = \frac{1}{4} (I_4 + r_x \sigma_x \otimes \sigma_x + r_y \sigma_y \otimes \sigma_y + r_z \sigma_z \otimes \sigma_z), \quad (\text{C16})$$

where I_4 denotes a 4×4 identity matrix, the reduced density matrix can be easily calculated as

$$\rho_A = \rho_B = \frac{1}{2} I_2. \quad (\text{C17})$$

Thus we have

$$\text{tr} \rho_{AB}^2 = \frac{1}{4} (1 + r_x^2 + r_y^2 + r_z^2), \quad \text{tr} \rho_A^2 = \text{tr} \rho_B^2 = \frac{1}{2}, \quad \text{tr}[\rho_{AB}(\rho_A \otimes \rho_B)] = \frac{1}{4}. \quad (\text{C18})$$

Then both the entropy criterion and the T_2 criterion indicate entanglement for

$$r_x^2 + r_y^2 + r_z^2 \geq 1. \quad (\text{C19})$$

Then we take

$$\rho_{AB} = (1-p)|\Psi^+\rangle\langle\Psi^+| + p|0+\rangle\langle 0+|, \quad (\text{C20})$$

a mixture of the two-qubit maximally entangled state and the tensor product of $|0\rangle\langle 0|$ and $|+\rangle\langle +|$, as an example to demonstrate the detection power of the T_2 separability criterion. For comparison, we pick three commonly used separability criteria:

1. PPT criterion, $W(p) = -\min\{\lambda(\rho_{AB}^{T_B})\}$
2. entropy criterion, $W(p) = \text{tr} \rho_{AB}^2 - \text{tr} \rho_A^2$
3. p_3 -PPT criterion, $W(p) = (\text{tr} \rho_{AB}^2)^2 - \text{tr}(\rho_{AB}^{T_B})^3$

and T_2 criterion, $W(p) = \text{tr} \rho_{AB}^2 + \text{tr} \rho_A^2 + \text{tr} \rho_B^2 - 2 \text{tr}[\rho_{AB}(\rho_A \otimes \rho_B)] - 1$, show them in one diagram. For these four criteria, $W(p) > 0$ indicates entanglement and the absolute value of $W(p)$ makes no sense. As shown in Fig. 8, for states in Eq. (C20), the T_2 criterion shows the same detection power as the PPT criterion, the necessary and sufficient separability condition for 2×2 states, and better than the p_3 -PPT criterion and entropy criterion.

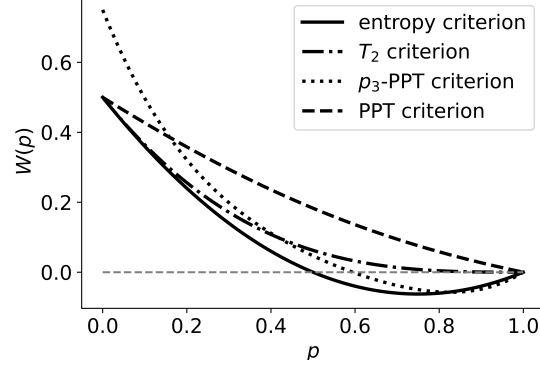


FIG. 8. Comparison of the detection power of four separability criteria for states in Eq. (C20).

Appendix D: A few Proofs

1. Proof of Eq. (10)

The result in Eq. (10) was derived in Refs. [31, 52]. Here we prove it for completeness. According to the Weingarten integral introduced in Appendix A1,

$$\begin{aligned}
\Phi_2(X) &= \sum_{\pi, \sigma \in \mathcal{S}_2} C_{\pi, \sigma} \text{tr}(W_\pi X) W_\sigma \\
&= \sum_{\pi, \sigma \in \mathcal{S}_2} \sum_{s, s'} C_{\pi, \sigma} - (-d)^{\delta_{s, s'}} \text{tr}(W_\pi |s, s'\rangle \langle s, s'|) W_\sigma \\
&= \sum_{s, s'} -(-d)^{\delta_{s, s'}} \{ [C_{0,0} \text{tr}(I|s, s'\rangle \langle s, s'|) + C_{1,0} \text{tr}(S|s, s'\rangle \langle s, s'|)] I + [C_{0,1} \text{tr}(I|s, s'\rangle \langle s, s'|) + C_{1,1} \text{tr}(S|s, s'\rangle \langle s, s'|)] S \} \\
&= \sum_{s, s'} d(-d)^{\delta_{s, s'}-1} \left\{ \left[\frac{1}{d^2-1} - \frac{1}{d(d^2-1)} \delta_{s, s'} \right] I + \left[-\frac{1}{d(d^2-1)} + \frac{1}{d^2-1} \delta_{s, s'} \right] S \right\} \\
&= \sum_{s, s'} \left\{ \left[-\frac{1}{d^2-1} + \frac{d}{d^2-1} \delta_{s, s'} \right] I + \left[\frac{1}{d(d^2-1)} + \frac{d^2-d-1}{d(d^2-1)} \delta_{s, s'} \right] S \right\} \\
&= \left\{ \left[-\frac{d^2}{d^2-1} + \frac{d^2}{d^2-1} \right] I + \left[\frac{d^2}{d(d^2-1)} + \frac{d^3-d^2-d}{d(d^2-1)} \right] S \right\} \\
&= S
\end{aligned} \tag{D1}$$

Here in the third line, for simplicity, we use 0 and 1 to represent identity and exchange in the subscript of Weingarten matrix element $C_{\pi, \sigma}$. The fifth equal sign is because

$$-(-d)^{\delta_{s, s'}} = -1 + (d+1)\delta_{s, s'}, \tag{D2}$$

and the sixth equal sign is because

$$\sum_{s, s'} 1 = d^2, \quad \sum_{s, s'} \delta_{s, s'} = d \tag{D3}$$

2. Proof of Proposition 1

By Born's rule,

$$\begin{aligned} \Pr(s|U) &= \text{tr} \left[|s_{g_1}, \dots, s_{g_k}\rangle \langle s_{g_1}, \dots, s_{g_k}| \left(\bigotimes_{i=1}^k U_{g_i} \right) \rho \left(\bigotimes_{i=1}^k U_{g_i} \right)^\dagger \right] \\ \Pr(s_{g_i}|U_{g_i}) &= \text{tr} (|s_{g_i}\rangle \langle s_{g_i}| U_{g_i} \rho_{g_i} U_{g_i}^\dagger) \end{aligned} \quad (\text{D4})$$

The right-hand side of Eq. (8) can be written as

$$\begin{aligned} \text{RHS} &= \text{tr} \left\{ \left(\bigotimes_{i=1}^k X_{g_i} \right) \mathbb{E}_U \left[\left(\bigotimes_{i=1}^k U_{g_i} \right)^{\otimes 2} \left[\rho \otimes \left(\bigotimes_{i=1}^k \rho_{g_i} \right) \right] \left(\bigotimes_{i=1}^k U_{g_i} \right)^{\dagger \otimes 2} \right] \right\} \\ &= \text{tr} \left\{ \mathbb{E}_U \left[\left(\bigotimes_{i=1}^k U_{g_i} \right)^{\dagger \otimes 2} \left(\bigotimes_{i=1}^k X_{g_i} \right) \left(\bigotimes_{i=1}^k U_{g_i} \right)^{\otimes 2} \right] \left[\rho \otimes \left(\bigotimes_{i=1}^k \rho_{g_i} \right) \right] \right\} \\ &= \text{tr} \left\{ \left[\bigotimes_{i=1}^k \Phi_{g_i}^{\dagger 2}(X_{g_i}) \right] \left[\rho \otimes \left(\bigotimes_{i=1}^k \rho_{g_i} \right) \right] \right\}, \end{aligned} \quad (\text{D5})$$

where X_{g_i} follows the same definition as the X in Eq. (10), and $\tilde{\Phi}^2(\cdot) = \mathbb{E}_U[U^\dagger \cdot U]$. For arbitrary linear operator A and B , we have:

$$\text{tr} [\Phi^{\dagger k}(A)B] = \text{tr} [A\Phi^k(B)] = \sum_{\pi, \sigma \in \mathcal{S}_k} C_{\pi, \sigma} \text{tr}(W_\pi B) \text{tr}(W_\sigma A) \quad (\text{D6})$$

So, when taking trace, it is always true that

$$\Phi^{\dagger k}(A) = \sum_{\pi, \sigma \in \mathcal{S}_k} C_{\pi, \sigma} \text{tr}(W_\sigma A) W_\pi. \quad (\text{D7})$$

Since $C_{\pi, \sigma} = C_{\sigma, \pi}$ [69],

$$\Phi^{\dagger k}(A) = \sum_{\pi, \sigma \in \mathcal{S}_k} C_{\pi, \sigma} \text{tr}(W_\pi A) W_\sigma = \Phi^k(A), \quad (\text{D8})$$

so that

$$\begin{aligned} \text{RHS} &= \text{tr} \left\{ \left[\bigotimes_{i=1}^k \Phi_{g_i}^{\dagger 2}(X_{g_i}) \right] \left[\rho \otimes \left(\bigotimes_{i=1}^k \rho_{g_i} \right) \right] \right\} \\ &= \text{tr} \left\{ \left(\bigotimes_{i=1}^k S_{g_i} \right) \left[\rho \otimes \left(\bigotimes_{i=1}^k \rho_{g_i} \right) \right] \right\} \\ &= \text{tr} \left[\rho \left(\bigotimes_{i=1}^k \rho_{g_i} \right) \right] = T_k. \end{aligned} \quad (\text{D9})$$

3. Proof of Proposition 2

The proof of local protocol is quite similar with global protocol. According to Eq. (13), define the data processing operator:

$$\tilde{X}_{g_i} = \sum_{\vec{s}_{g_i}, \vec{s}'_{g_i}} \tilde{X}_{g_i}(\vec{s}_{g_i}, \vec{s}'_{g_i}) |\vec{s}_{g_i}, \vec{s}'_{g_i}\rangle \langle \vec{s}_{g_i}, \vec{s}'_{g_i}| = \bigotimes_{l \in g_i} X_l. \quad (\text{D10})$$

Substituting this operator into Eq. (12), the right hand side can be written as

$$\begin{aligned}
\text{RHS} &= \text{tr} \left\{ \left(\bigotimes_{i=1}^k \tilde{X}_{g_i} \right) \mathbb{E}_U \left[\left(\bigotimes_{l=1}^n U_l \right)^{\otimes 2} \left[\rho \otimes \left(\bigotimes_{i=1}^k \rho_{g_i} \right) \right] \left(\bigotimes_{l=1}^n U_l \right)^{\dagger \otimes 2} \right] \right\} \\
&= \text{tr} \left\{ \mathbb{E}_U \left[\left(\bigotimes_{l=1}^n U_l \right)^{\dagger \otimes 2} \left(\bigotimes_{l=1}^n X_l \right) \left(\bigotimes_{l=1}^n U_l \right)^{\otimes 2} \right] \left[\rho \otimes \left(\bigotimes_{i=1}^k \rho_{g_i} \right) \right] \right\} \\
&= \text{tr} \left\{ \left(\bigotimes_{l=1}^n \Phi^{\dagger 2}(X_l) \right) \left[\rho \otimes \left(\bigotimes_{i=1}^k \rho_{g_i} \right) \right] \right\} \\
&= \text{tr} \left\{ \left(\bigotimes_{l=1}^n S_l \right) \left[\rho \otimes \left(\bigotimes_{i=1}^k \rho_{g_i} \right) \right] \right\} \\
&= \text{tr} \left[\rho \left(\bigotimes_{i=1}^k \rho_{g_i} \right) \right] = T_k.
\end{aligned} \tag{D11}$$

Appendix E: The variance of \hat{M} and \hat{M}_L

1. The variance of \hat{M}

In the following, we figure out the variance $\delta^2 \doteq \mathbf{Var} \left[\hat{M}(t) \right]$ of the estimator $\hat{M}(t)$ for the t -th unitary sampling. The variance of the overall estimator \hat{M} is just δ^2/N_U . Hereafter, for the convenience of our analysis, we take tripartite CRO, T_3 , as an example to analyze the error scaling and assume that the unitary ensembles are 4-design. The results for T_3 can be easily generalized to T_k and the 4-design assumption would not lead to an order of magnitude gap of the leading term.

With the total variance formula, we have

$$\mathbf{Var} \left[\hat{M}(t) \right] = \mathbb{E}_U \left[\mathbb{E}_{\mathbf{s}} \left[\hat{M}^2(t) | U \right] \right] - \left[\mathbb{E}_U \mathbb{E}_{\mathbf{s}} \left[\hat{M}(t) | U \right] \right]^2, \tag{E1}$$

where the second term is just T_3^2 . The first term can be expanded explicitly as

$$\mathbb{E}_U \left[\mathbb{E}_{\mathbf{s}} \left[\hat{M}^2(t) | U \right] \right] = \binom{N_M}{4}^{-2} \sum_{\substack{i < j < k < l \\ i' < j' < k' < l'}} \mathbb{E}_{\mathbf{s}, U} \text{tr} [Q \hat{r}_U(i) \otimes \hat{r}_U(j) \otimes \hat{r}_U(k) \otimes \hat{r}_U(l)] \text{tr} [Q \hat{r}_U(i') \otimes \hat{r}_U(j') \otimes \hat{r}_U(k') \otimes \hat{r}_U(l')]. \tag{E2}$$

To evaluate the above equation, we calculate the terms in the summation depending on the coincidence of the indices, as they label random variables. In Appendix F, we will show that when $D \gg N_M \gg 1$, which is the case of interest, the dominant term of the variance is determined by the case when all the eight indices are coincidental to four indices. This kind of phenomenon is also manifested by the previous theoretical and numerical analyses [35, 36, 51] for other quantities based on randomized measurements.

$$\begin{aligned}
\Gamma_4 &:= \binom{N_M}{4}^{-2} \sum_{\substack{i=i' < j=j' \\ < k=k' < l=l'}} \mathbb{E}_{\mathbf{s}, U} \text{tr} [Q \hat{r}_U(i) \otimes \hat{r}_U(j) \otimes \hat{r}_U(k) \otimes \hat{r}_U(l)] \text{tr} [Q \hat{r}_U(i') \otimes \hat{r}_U(j') \otimes \hat{r}_U(k') \otimes \hat{r}_U(l')] \\
&= \binom{N_M}{4}^{-1} \mathbb{E}_{\mathbf{s}, U} \text{tr} [Q^2 \hat{r}_U(i) \otimes \hat{r}_U(j) \otimes \hat{r}_U(k) \otimes \hat{r}_U(l)] \\
&= \binom{N_M}{4}^{-1} \text{tr} [Q^2 \Phi_A^4 \otimes \Phi_B^4 \otimes \Phi_C^4 (\rho_{ABC}^{\otimes 4})] \\
&= \binom{N_M}{4}^{-1} \text{tr} [\Phi_A^4 \otimes \Phi_B^4 \otimes \Phi_C^4 (Q^2) \rho_{ABC}^{\otimes 4}] \\
&= \binom{N_M}{4}^{-1} \text{tr} [\Phi_A^{(1,2)} \otimes \Phi_B^{(1,3)} \otimes \Phi_C^{(1,4)} (Q^2) \rho_{ABC}^{\otimes 4}].
\end{aligned} \tag{E3}$$

Here, $\Phi_A^{(i,j)}(\cdot) := \mathbb{E}_{U_A} (U_A^{(i)} \otimes U_A^{(j)}) \cdot (U_A^{(i)} \otimes U_A^{(j)})^\dagger$ denotes the twofold twirling on subsystems A of the i -th and j -th copies, similar for $\Phi_B^{(i,j)}(\cdot)$ and $\Phi_C^{(i,j)}(\cdot)$. The last equation of Eq. (E3) holds because the observable Q only has nontrivial definitions on the systems A_1, A_2, B_1, B_3, C_1 and C_4 as follows

$$Q = \left(X_A^{(1,2)} \otimes I_A^{(3,4)} \right) \otimes \left(X_B^{(1,3)} \otimes I_B^{(2,4)} \right) \otimes \left(X_C^{(1,4)} \otimes I_C^{(2,3)} \right). \quad (\text{E4})$$

Using the Weingarten integral [69], we can get

$$\Phi_A^{(1,2)}[(X_A^{(1,2)})^2] = d_A I_A^{(1,2)} + (d_A - 1) S_A^{(1,2)}, \quad (\text{E5})$$

thus Γ_4 shows

$$\Gamma_4 := \binom{N_M}{4}^{-1} \text{tr} \left[\left(d_A I_A + (d_A - 1) S_A^{(1,2)} \right) \left(d_B I_B + (d_B - 1) S_B^{(1,3)} \right) \left(d_C I_C + (d_C - 1) S_C^{(1,3)} \right) \rho_{ABC}^{\otimes 4} \right] \quad (\text{E6})$$

It is clear that Γ_4 depends on the input state ρ_{ABC} . By expanding Eq. (E6), one gets a few functions of ρ_{ABC} , with the coefficients almost D . For example,

$$\begin{aligned} \text{tr} \left[(d_A I_A d_B I_B d_C I_C) \rho_{ABC}^{\otimes 4} \right] &= d_A d_B d_C = D, \\ \text{tr} \left[\left((d_A - 1) S_A^{(1,2)} \otimes (d_B - 1) S_B^{(1,3)} \otimes (d_C - 1) S_C^{(1,3)} \right) \rho_{ABC}^{\otimes 4} \right] &= (d_A - 1)(d_B - 1)(d_C - 1) T_3 \leq D. \end{aligned} \quad (\text{E7})$$

The term Γ_4 scales up linearly with D . As a result, the variance $\delta^2 \sim \Theta(D)$.

Here, we take T_3 as an example to demonstrate our results. In fact, this conclusion can easily be generalized to T_k measurement for any value of k . Following the similar thought in Appendix F, we believe that the leading term is also the one which has $(k+1)$ pairs of the same indices, like Γ_4 in T_3 measurement. So the dominant term of variance when measuring T_k is

$$\Gamma_{k+1} = \binom{N_M}{k+1}^{-1} \text{tr} \left[\bigotimes_{i=1}^k \left(d_i I_i + (d_i - 1) S_i^{(1,i+1)} \right) \rho^{\otimes k+1} \right] \sim \Theta(D/N_M^{k+1}) \quad (\text{E8})$$

2. The unbiased estimator \hat{M}_L and its variance

In the above derivation, we consider the variance calculation when the random unitaries $U = U_A \otimes U_B \otimes U_C$ are chosen such that $U_A, U_B,$ and U_C are elements of unitary 2-design on the corresponding Hilbert spaces. Now we consider the variance estimation in the local strategy mentioned in Sec. III, when the subsystems $A, B,$ and C are composed of qubits. In this case, the random unitary twirling is performed locally on each qubit. From Eq. (12), we can express the tripartite correlation as follows:

$$T_3 = \sum_{\vec{a}, \vec{b}, \vec{c}} \tilde{X}_A^{(1,2)}(\vec{a}^1, \vec{a}^2) \tilde{X}_B^{(1,3)}(\vec{b}^1, \vec{b}^3) \tilde{X}_C^{(1,4)}(\vec{c}^1, \vec{c}^4) \prod_{i=1}^4 \mathbb{E} \Pr(\vec{a}^i, \vec{b}^i, \vec{c}^i | U_A, U_B, U_C), \quad (\text{E9})$$

where $\vec{a} = (\vec{a}^1, \vec{a}^2, \vec{a}^3, \vec{a}^4)$ denotes the measurement result, being a string whose elements are n_A -bit vectors, similar for \vec{b} and \vec{c} . $\tilde{X}_A^{(1,2)}(\vec{a}^1, \vec{a}^2)$ is a function on \vec{a}^1 and \vec{a}^2 ,

$$\tilde{X}_A^{(1,2)}(\vec{a}^1, \vec{a}^2) := \prod_{i=1}^{n_A} X_{A_i}^{(1,2)}(a_i^1, a_i^2) = 2^{n_A} (-2)^{-D[\vec{a}^1, \vec{a}^2]}. \quad (\text{E10})$$

We also denote $\tilde{X}_A^{(1,2)}$ as the observable on $\mathcal{H}_A^1 \otimes \mathcal{H}_A^2$,

$$\tilde{X}_A^{1,2} = \sum_{\vec{a}^1, \vec{a}^2} \tilde{X}_A^{(1,2)}(\vec{a}^1, \vec{a}^2) |\vec{a}^1, \vec{a}^2\rangle \langle \vec{a}^1, \vec{a}^2|. \quad (\text{E11})$$

similar for $\tilde{X}_B^{(1,3)}$ and $\tilde{X}_C^{(1,4)}$. Similar to Eq. (17), we can define the unbiased estimator based on the local random unitary scheme,

$$\hat{M}_L(t) = \binom{N_M}{4}^{-1} \sum_{1 \leq i < j < k < l \leq N_M} \text{tr} \left[\tilde{Q} [\hat{r}_U(i) \otimes \hat{r}_U(j) \otimes \hat{r}_U(k) \otimes \hat{r}_U(l)] \right], \quad (\text{E12})$$

where

$$\tilde{Q} := \left(\tilde{X}_A^{(1,2)} \otimes I_A^{(3,4)} \right) \otimes \left(\tilde{X}_B^{(1,3)} \otimes I_B^{(2,4)} \right) \otimes \left(\tilde{X}_C^{(1,4)} \otimes I_C^{(2,3)} \right), \quad (\text{E13})$$

is an observable on $\mathcal{H}^{\otimes 4}$.

Following the same deduction, to calculate the variance of $\hat{M}_L(t)$, we evaluate the leading term with four coincidences

$$\begin{aligned} \tilde{\Gamma}_4 &:= \binom{N_M}{4}^{-2} \sum_{\substack{i=i' < j=j' \\ < k=k' < l=l'}} \mathbb{E}_{\mathbf{s}, U} \text{tr} \left[\tilde{Q} \hat{r}_U(i) \otimes \hat{r}_U(j) \otimes \hat{r}_U(k) \otimes \hat{r}_U(l) \right] \text{tr} \left[\tilde{Q} \hat{r}_U(i') \otimes \hat{r}_U(j') \otimes \hat{r}_U(k') \otimes \hat{r}_U(l') \right] \\ &= \binom{N_M}{4}^{-1} \mathbb{E}_{\mathbf{s}, U} \text{tr} \left[\tilde{Q}^2 \hat{r}_U(i) \otimes \hat{r}_U(j) \otimes \hat{r}_U(k) \otimes \hat{r}_U(l) \right] \\ &= \binom{N_M}{4}^{-1} \text{tr} \left[\tilde{\Phi}_A^4 \otimes \tilde{\Phi}_B^4 \otimes \tilde{\Phi}_C^4 (\tilde{Q}^2) \rho_{ABC}^{\otimes 4} \right] \\ &= \binom{N_M}{4}^{-1} \text{tr} \left[\tilde{\Phi}_A^{(1,2)} \otimes \tilde{\Phi}_B^{(1,3)} \otimes \tilde{\Phi}_C^{(1,4)} (\tilde{Q}^2) \rho_{ABC}^{\otimes 4} \right]. \end{aligned} \quad (\text{E14})$$

The final line is because \tilde{Q} acts nontrivially on the systems A_1, A_2, B_1, B_3, C_1 and C_4 . The only difference compared to Eq. (E3) is that both the twirling channels $\tilde{\Phi}_A^{(1,2)}$ and $\tilde{Q}_A^{(1,2)}$ have the tensor-product structure on qubits,

$$\tilde{\Phi}_A^{(1,2)} [(\tilde{Q}_A^{(1,2)})^2] = \bigotimes_{i \in A} \Phi_i^{(1,2)} [(X_i^{(1,2)})^2] = \bigotimes_{i \in A} (2I_i + S_i^{(1,2)}), \quad (\text{E15})$$

similar for operators on B and C , and thus $\tilde{\Gamma}_4$ shows

$$\begin{aligned} \tilde{\Gamma}_4 &:= \binom{N_M}{4}^{-1} \text{tr} \left[\bigotimes_{i \in A} (2I_i + S_i^{(1,2)}) \bigotimes_{j \in B} (2I_j + S_j^{(1,3)}) \bigotimes_{k \in C} (2I_k + S_k^{(1,4)}) \rho_{ABC}^{\otimes 4} \right] \\ &= \binom{N_M}{4}^{-1} \sum_{A' \subseteq A, B' \subseteq B, C' \subseteq C} 2^{|A|-|A'|} 2^{|B|-|B'|} 2^{|C|-|C'|} \text{tr} [\rho_{A'B'C'} (\rho_{A'} \otimes \rho_{B'} \otimes \rho_{C'})] \\ &\leq \binom{N_M}{4}^{-1} \sum_{A' \subseteq A, B' \subseteq B, C' \subseteq C} 2^n 2^{-|A'|} 2^{-|B'|} 2^{-|C'|} \\ &= \binom{N_M}{4}^{-1} \sum_{|A'|, |B'|, |C'|} \binom{|A|}{|A'|} \binom{|B|}{|B'|} \binom{|C|}{|C'|} 2^n 2^{-|A'|} 2^{-|B'|} 2^{-|C'|} = \binom{N_M}{4}^{-1} 2^n \left(1 + \frac{1}{2}\right)^{n_A + n_B + n_C} = \binom{N_M}{4}^{-1} 3^n. \end{aligned} \quad (\text{E16})$$

Here in the second line, we expand the terms and the summation of A' runs for all subsets of A including the null set. For example, if $A = \emptyset$, $\text{tr} [\rho_{A'B'C'} (\rho_{A'} \otimes \rho_{B'} \otimes \rho_{C'})] = \text{tr} [\rho_{B'C'} (\rho_{B'} \otimes \rho_{C'})]$. The inequality is due to the overlap is less than 1. As a result, the term $\tilde{\Gamma}_4$ is upper bounded by $\binom{N_M}{4}^{-1} 3^n = \binom{N_M}{4}^{-1} D^{\log_2 3} \approx \binom{N_M}{4}^{-1} D^{1.585}$, and the the variance $\delta^2 \sim O(D^{1.585})$.

Similarly, the leading term of variance when measuring T_k scales like

$$\tilde{\Gamma}_{k+1} \leq \binom{N_M}{k+1}^{-1} 3^n \sim \frac{3^n}{N_M^{k+1}}. \quad (\text{E17})$$

Appendix F: Detailed statistical analysis

Here, we provide a detailed statistical analysis of the estimation of the tripartite total correlation $\text{tr}[\rho_{ABC}(\rho_A \otimes \rho_B \otimes \rho_C)]$. For simplicity, we will consider the case when $d_A = d_B = d_C = d$. Then $D := d_A d_B d_C = d^3$.

Recall that we construct an estimator of T_3 using these variables in Eq. (17),

$$\hat{M}(t) = \binom{N_M}{4}^{-1} \sum_{1 \leq i < j < k < l \leq N_M} \text{tr} \{Q [\hat{r}_U(i) \otimes \hat{r}_U(j) \otimes \hat{r}_U(k) \otimes \hat{r}_U(l)]\}. \quad (\text{F1})$$

Now, we need to calculate the variance δ^2 of it. In the main text, we show that the core issue is to calculate the term,

$$\mathbb{E}_U \left[\mathbb{E}_s \left[\hat{M}_+^2(t) | U \right] \right] = \binom{N_M}{4}^{-2} \sum_{\substack{i < j < k < l \\ i' < j' < k' < l'}} \mathbb{E}_{s,U} \text{tr}[Q \hat{r}_U(i) \otimes \hat{r}_U(j) \otimes \hat{r}_U(k) \otimes \hat{r}_U(l)] \text{tr}[Q \hat{r}_U(i') \otimes \hat{r}_U(j') \otimes \hat{r}_U(k') \otimes \hat{r}_U(l')]. \quad (\text{F2})$$

Based on the coincident number of the sample indices $i, i'; j, j'; k, k'; l, l'$, we may classify the terms as follows,

1. No coincidence, i.e., the eight sample indices are all different. The number of their terms is

$$N_8 = \binom{N_M}{8} \binom{8}{0} \binom{8}{4}.$$

We denote the sum of these terms as Γ_8 .

2. One coincidence. In this case, we further classify the terms based on the coincident index:

- (a) The coincident indices are i and i' . The number of their terms is $N_7^{(2)} = \binom{N_M}{7} \binom{6}{3}$. We denote the sum of these terms as $\Gamma_7^{(2)}$.

- (b) One of the coincident indices is i or i' . The number of their terms is

$$N_7^{(1)} = \binom{N_M}{7} \left[\binom{6}{3} + 2 \binom{2}{2} \binom{4}{1} + 2 \binom{3}{3} \binom{3}{0} \right] = \binom{N_M}{7} \left[\binom{6}{3} + 10 \right].$$

We denote the sum of these terms as $\Gamma_7^{(1)}$.

- (c) None of the coincident indices is i or i' . The number of their terms is

$$N_7^{(0)} = \binom{N_M}{7} \left\{ \left[\binom{6}{3} - 2 \binom{2}{2} \binom{4}{1} \right] + \left[\binom{6}{3} - 2 \binom{3}{3} \binom{3}{0} \right] + 3 \binom{6}{3} \right\} = \binom{N_M}{7} \left(5 \binom{6}{3} - 10 \right).$$

We denote the sum of these terms as $\Gamma_7^{(0)}$.

3. Two coincidences. In this case, we also further classify the terms based on the coincident index:

- (a) The coincident indices contain both i and i' . The number of their terms is $N_6^{(2)} = \binom{N_M}{6} \binom{5}{1} \binom{4}{2}$. We denote the sum of these terms as $\Gamma_6^{(2)}$.

- (b) The coincident indices contain either i or i' . The number of their terms is

$$N_6^{(1)} = \binom{N_M}{6} \left[\binom{4}{1} \binom{4}{2} + 2 \binom{3}{1} \binom{2}{2} \binom{2}{0} \right] = \binom{N_M}{6} \left[\binom{4}{1} \binom{4}{2} + 6 \right].$$

We denote the sum of these terms as $\Gamma_6^{(1)}$.

- (c) The coincident indices do not contain i or i' . The number of their terms is

$$N_6^{(0)} = \binom{N_M}{6} \left\{ \binom{3}{1} \left[\binom{4}{2} - 2 \binom{2}{2} \right] + \binom{2}{1} \binom{4}{2} + \binom{1}{1} \binom{4}{2} \right\} = \binom{N_M}{6} \left\{ \left[\binom{3}{1} + \binom{2}{1} + \binom{1}{1} \right] \binom{4}{2} - 6 \right\}.$$

We denote the sum of these terms as $\Gamma_6^{(0)}$.

4. Three coincidences. In this case, we also further classify the terms based on the coincident index:

- (a) The coincident indices contain both i and i' . The number of their terms is $N_5^{(2)} = \binom{N_M}{5} \binom{4}{2} \binom{2}{1}$. We denote the sum of these terms as $\Gamma_5^{(2)}$.

- (b) The coincident indices contain either i or i' . The number of their terms is $N_5^{(1)} = \binom{N_M}{5} \binom{3}{2} \binom{2}{1}$. We denote the sum of these terms as $\Gamma_5^{(1)}$.

(c) The coincident indices do not contain i or i' . The number of their terms is $N_5^{(0)} = \binom{N_M}{5} \binom{2}{2} \binom{2}{1}$. We denote the sum of these terms as $\Gamma_5^{(0)}$.

5. Four coincidences, i.e., the eight sample indices collapse to four degenerated indices. The number of their terms is $N_4 = \binom{N_M}{4} \binom{4}{4} \binom{0}{0}$. We denote the sum of these terms as Γ_4 .

We can then expand the variance term as follows,

$$\mathbb{E}_U \left[\mathbb{E}_s \left[\hat{M}^2(t) | U \right] \right] = \Gamma_8 + \left(\Gamma_7^{(2)} + \Gamma_7^{(1)} + \Gamma_7^{(0)} \right) + \left(\Gamma_6^{(2)} + \Gamma_6^{(1)} + \Gamma_6^{(0)} \right) + \left(\Gamma_5^{(2)} + \Gamma_5^{(1)} + \Gamma_5^{(0)} \right) + \Gamma_4. \quad (\text{F3})$$

In what follows, we focus on the case when $D \gg N_M \gg 1$, which is the case of interest. We want to show that the term Γ_4 owns the highest dependence of the scaling of D .

Proposition 6. *When $D \gg N_M \gg 1$, in the tripartite total correlation estimation task, the different variance terms have the following dependence on the dimension D :*

$$\begin{aligned} \Gamma_8 &= O(1), \\ \Gamma_7^{(2)} &= O(1), \quad \Gamma_7^{(1)} = \Gamma_7^{(0)} = O(1), \\ \Gamma_6^{(2)} &= O(d) = O(D^{1/3}), \quad \Gamma_6^{(1)} = \Gamma_6^{(0)} = O(1), \\ \Gamma_5^{(2)} &= O(d^2) = O(D^{2/3}), \quad \Gamma_5^{(1)} = \Gamma_5^{(0)} = O(1), \\ \Gamma_4 &= \Theta(d^3) = \Theta(D). \end{aligned} \quad (\text{F4})$$

Proof. We will study the variance terms one by one.

$$\begin{aligned} & \binom{N_M}{4}^2 \binom{N_M}{8}^{-1} \binom{8}{4}^{-1} \Gamma_8 = \mathbb{E}_U \text{tr} [Q(\rho_U)^{\otimes 4}]^2 = \mathbb{E}_U \text{tr} [Q^{\otimes 2}(\rho_U)^{\otimes 8}] \\ &= \text{tr} \left[\rho^{\otimes 8} \Phi_A^{(1,2,5,6)} \left(X_A^{(1,2)} \otimes X_A^{(5,6)} \right) \otimes \Phi_B^{(1,3,5,7)} \left(X_B^{(1,3)} \otimes X_B^{(5,7)} \right) \otimes \Phi_C^{(1,4,5,8)} \left(X_C^{(1,4)} \otimes X_C^{(5,8)} \right) \right] \\ &= \sum_{\substack{\pi_1, \pi_2, \pi_3, \\ \sigma_1, \sigma_2, \sigma_3 \in S_4}} C_{\pi_1, \sigma_1} C_{\pi_2, \sigma_2} C_{\pi_3, \sigma_3} \text{tr} \left[\rho^{\otimes 8} \left(W_{\pi_1}^A \otimes W_{\pi_2}^B \otimes W_{\pi_3}^C \right) \right] \text{tr} \left[\left(X_A^{(1,2)} \otimes X_A^{(5,6)} \right) W_{\sigma_1}^A \right] \\ & \times \text{tr} \left[\left(X_B^{(1,3)} \otimes X_B^{(5,7)} \right) W_{\sigma_2}^B \right] \text{tr} \left[\left(X_C^{(1,4)} \otimes X_C^{(5,8)} \right) W_{\sigma_3}^C \right] \end{aligned} \quad (\text{F5})$$

Here, $\rho_U := U \rho U^\dagger$. In the third equality, we assume the random unitaries form a unitary 4-design. In the fourth equality, we use the Weingarten integral formula [69].

The value of Γ_8 is obviously state dependent. However, when we consider the asymptotic case when $d \gg N_M \gg 1$, to analyze the scaling of Γ_8 with d , we always consider a *pure tensor state* $\rho = |\psi\rangle_A \langle \psi| \otimes |\psi\rangle_B \langle \psi| \otimes |\psi\rangle_C \langle \psi|$. In this case, the values

$$\text{tr} \left[\rho^{\otimes 8} \left(W_{\pi_1}^A \otimes W_{\pi_2}^B \otimes W_{\pi_3}^C \right) \right] \quad (\text{F6})$$

are always 1. We remark that, if ρ is not a pure tensor state, the absolute value of this term is always smaller than 1. From this perspective, the pure-tensor-state case will always provide an upper bound of the variance term dependence.

If we set the state ρ to be a pure tensor state, then we have

$$\begin{aligned}
& \binom{N_M}{4}^2 \binom{N_M}{8}^{-1} \binom{8}{4}^{-1} \Gamma_8 \\
&= \sum_{\substack{\pi_1, \pi_2, \pi_3, \\ \sigma_1, \sigma_2, \sigma_3 \in S_4}} C_{\pi_1, \sigma_1} C_{\pi_2, \sigma_2} C_{\pi_3, \sigma_3} \operatorname{tr} \left[\left(X_A^{(1,2)} \otimes X_A^{(5,6)} \right) W_{\sigma_1}^A \right] \operatorname{tr} \left[\left(X_B^{(1,3)} \otimes X_B^{(5,7)} \right) W_{\sigma_2}^B \right] \operatorname{tr} \left[\left(X_C^{(1,4)} \otimes X_C^{(5,8)} \right) W_{\sigma_3}^C \right] \\
&= \sum_{\sigma_1, \sigma_2, \sigma_3 \in S_4} \operatorname{tr} \left[\left(X_A^{(1,2)} \otimes X_A^{(5,6)} \right) W_{\sigma_1}^A \right] \operatorname{tr} \left[\left(X_B^{(1,3)} \otimes X_B^{(5,7)} \right) W_{\sigma_2}^B \right] \operatorname{tr} \left[\left(X_C^{(1,4)} \otimes X_C^{(5,8)} \right) W_{\sigma_3}^C \right] \\
&\times \sum_{\pi_1, \pi_2, \pi_3 \in S_4} C_{\pi_1, \sigma_1} C_{\pi_2, \sigma_2} C_{\pi_3, \sigma_3} \\
&= \left\{ \sum_{\sigma_1 \in S_4} \operatorname{tr} \left[\left(X_A^{(1,2)} \otimes X_A^{(5,6)} \right) W_{\sigma_1}^A \right] \sum_{\pi_1 \in S_4} C_{\pi_1, \sigma_1} \right\}^3 \\
&= \left\{ \frac{(d-1)!}{(d+3)!} \sum_{\sigma \in S_4} \operatorname{tr} \left[\left(X_A^{\otimes 2} \right) W_{\sigma}^A \right] \right\}^3 \\
&= \left\{ \frac{(d-1)!}{(d+3)!} d(d+1)(d^2+9d+2) \right\}^3.
\end{aligned} \tag{F7}$$

In the last equation, we have used Proposition 7. Therefore, $\Gamma_8 \sim O(1)$.

Following similar methods, if we assume the state to be a pure tensor state, we can prove that

$$\begin{aligned}
\frac{1}{N_7^{(2)}} \binom{N_M}{4}^2 \Gamma_7^{(2)} &= \left\{ \frac{(d-1)!}{(d+2)!} \sum_{\sigma \in S_3} \operatorname{tr} \left[\left(X_A^{(12,13)} \right) W_{\sigma}^A \right] \right\}^3 \\
&= \left\{ \frac{(d-1)!}{(d+2)!} 3d^2(d+1) \right\}^3 \sim O(1)
\end{aligned} \tag{F8}$$

$$\begin{aligned}
\frac{1}{N_7^{(1)}} \binom{N_M}{4}^2 \Gamma_7^{(1)} &= \frac{1}{N_7^{(0)}} \binom{N_M}{4}^2 \Gamma_7^{(0)} \\
&= \left\{ \frac{(d-1)!}{(d+2)!} \sum_{\sigma \in S_3} \operatorname{tr} \left[\left(X_A^{(12,13)} \right) W_{\sigma}^A \right] \right\} \left\{ \frac{(d-1)!}{(d+3)!} \sum_{\sigma \in S_4} \operatorname{tr} \left[\left(X_A^{\otimes 2} \right) W_{\sigma}^A \right] \right\}^2 \\
&= \left\{ \frac{(d-1)!}{(d+2)!} 3d^2(d+1) \right\} \left\{ \frac{(d-1)!}{(d+3)!} d(d+1)(d^2+9d+2) \right\}^2 \sim O(1)
\end{aligned} \tag{F9}$$

$$\begin{aligned}
\frac{1}{N_6^{(2)}} \binom{N_M}{4}^2 \Gamma_6^{(2)} &= \left\{ \frac{(d-1)!}{(d+2)!} \sum_{\sigma \in S_3} \operatorname{tr} \left[\left(X_A^{(12,13)} \right) W_{\sigma}^A \right] \right\}^2 \left\{ \frac{(d-1)!}{(d+1)!} \sum_{\sigma \in S_2} \operatorname{tr} \left[X_A^2 W_{\sigma}^A \right] \right\} \\
&= \left\{ \frac{(d-1)!}{(d+2)!} 3d^2(d+1) \right\}^2 \left\{ \frac{(d-1)!}{(d+1)!} d(2d-1)(d+1) \right\} \sim O(d) = O(D^{1/3})
\end{aligned} \tag{F10}$$

$$\begin{aligned}
\frac{1}{N_6^{(1)}} \binom{N_M}{4}^2 \Gamma_6^{(1)} &= \frac{1}{N_6^{(0)}} \binom{N_M}{4}^2 \Gamma_6^{(0)} \\
&= \left\{ \frac{(d-1)!}{(d+2)!} \sum_{\sigma \in S_3} \operatorname{tr} \left[\left(X_A^{(12,13)} \right) W_{\sigma}^A \right] \right\}^3 \\
&= \left\{ \frac{(d-1)!}{(d+2)!} 3d^2(d+1) \right\}^3 \sim O(1)
\end{aligned} \tag{F11}$$

$$\begin{aligned}
& \frac{1}{N_5^{(2)}} \binom{N_M}{4}^2 \Gamma_5^{(2)} \\
&= \left\{ \frac{(d-1)!}{(d+2)!} \sum_{\sigma \in S_3} \text{tr} \left[\left(X_A^{(12,13)} \right) W_\sigma^A \right] \right\} \left\{ \frac{(d-1)!}{(d+1)!} \sum_{\sigma \in S_2} \text{tr} \left[X_A^2 W_\sigma^A \right] \right\}^2 \\
&= \left\{ \frac{(d-1)!}{(d+2)!} 3d^2(d+1) \right\} \left\{ \frac{(d-1)!}{(d+1)!} d(2d-1)(d+1) \right\}^2 \sim O(d^2) = O(D^{2/3})
\end{aligned} \tag{F12}$$

$$\begin{aligned}
& \frac{1}{N_5^{(1)}} \binom{N_M}{4}^2 \Gamma_5^{(1)} = \frac{1}{N_5^{(0)}} \binom{N_M}{4}^2 \Gamma_5^{(0)} \\
&= \left\{ \frac{(d-1)!}{(d+2)!} \sum_{\sigma \in S_3} \text{tr} \left[\left(X_A^{(12,13)} \right) W_\sigma^A \right] \right\}^3 \\
&= \left\{ \frac{(d-1)!}{(d+2)!} 3d^2(d+1) \right\}^3 \sim O(1)
\end{aligned} \tag{F13}$$

The term Γ_4 has already been calculated in Eq. (E6), which is

$$\Gamma_4 = \binom{N_M}{4}^{-1} \text{tr} \left[\left(dI_A + (d-1)S_A^{(1,2)} \right) \left(dI_B + (d-1)S_B^{(1,3)} \right) \left(dI_C + (d-1)S_C^{(1,3)} \right) \rho_{ABC}^{\otimes 4} \right] \sim \Theta(D). \tag{F14}$$

□

In the above proofs, we have used the following results.

Proposition 7. For the observables defined on several copies of \mathcal{H}_A ,

$$\begin{aligned}
X^2 &= \sum_{\mathbf{a} \in \mathbb{Z}_d^2} X^2(a^1, a^2) |a^1, a^2\rangle \langle a^1, a^2|, \\
X^{(12,13)} &= \sum_{\mathbf{a} \in \mathbb{Z}_d^3} X(a^1, a^2) X(a^1, a^3) |a^1, a^2, a^3\rangle \langle a^1, a^2, a^3|, \\
X^{\otimes 2} &= \sum_{\mathbf{a} \in \mathbb{Z}_d^4} X(a^1, a^2) X(a^3, a^4) |a^1, a^2, a^3, a^4\rangle \langle a^1, a^2, a^3, a^4|,
\end{aligned} \tag{F15}$$

where $X(a^1, a^2) = -(-d)^{\delta_{a^1, a^2}}$. When the dimension of \mathcal{H}_A is d , we have

$$\begin{aligned}
& \sum_{\sigma \in S_2} \text{tr}(W_\sigma X^2) = d(2d-1)(d+1), \\
& \sum_{\sigma \in S_3} \text{tr}(W_\sigma X^{(12,13)}) = 3d^2(d+1), \\
& \sum_{\sigma \in S_4} \text{tr}(W_\sigma X^{\otimes 2}) = d(d+1)(d^2 + 9d + 2).
\end{aligned} \tag{F16}$$

Proof. First we note that,

$$\begin{aligned}
& \sum_{\sigma \in S_2} \text{tr}(W_\sigma X^2) = \text{tr}[(I + S)X^2] \\
&= \sum_{a^1, a^2} d^2 (d^2)^{\delta_{[a^1, a^2]} - 1} \langle a^1, a^2 | (I + S) | a^1, a^2 \rangle \\
&= 2d^3 + d^2 - d \sim O(d^3).
\end{aligned} \tag{F17}$$

Then we consider the term for $X^{(12,13)}$. Following the analysis in Ref. [36], we denote the cycle structures (conjugate classes) of the elements $\sigma \in S_t$ using the partition numbers $[\xi_1, \xi_2, \dots, \xi_k]$ where $\xi_1 \geq \xi_2 \geq \dots \geq \xi_k \geq 0$. Also, we can classify t -dit strings \mathbf{a} by the partition numbers $\lambda \mathbf{a}$. For example, the partition number $\lambda(\mathbf{a})$ of $\mathbf{a} = (1, 2, 1)$ is $[2, 1]$.

After classifying the cycle structure of the elements in S_t , for a diagonal observable Q in the Hilbert space $\mathcal{H}_A^{\otimes t}$, we have

$$\sum_{\pi \in S_t} \text{tr}(W_\pi Q) = \sum_{\mathbf{a} \in \mathbb{Z}_d^t} Q(\mathbf{a}) \sum_{\pi \in S_t} \langle \mathbf{a} | W_\pi | \mathbf{a} \rangle = \sum_{\mathbf{a} \in \mathbb{Z}_d^t} Q(\mathbf{a}) T(\mathbf{a}), \quad (\text{F18})$$

where

$$T(\mathbf{a}) = \sum_{\pi \in S_t} \text{tr}(W_\pi | \mathbf{a} \rangle \langle \mathbf{a} |) = \prod_{i=1}^k (\lambda_i(\mathbf{a})!). \quad (\text{F19})$$

The value of $T(\mathbf{a})$ only depends on the cycle structure of \mathbf{a} , i.e., how many values in \mathbf{a} are the same.

Furthermore, to calculate $\sum_{\mathbf{a} \in \mathbb{Z}_d^t} Q(\mathbf{a}) T(\mathbf{a})$, we first classify all the t -dit strings $\mathbf{a} \in \mathbb{Z}_d^t$ by their partitions $\lambda \mathbf{a}$, and then further divide them by the weight of the subsystems. By counting the weight of the subsystems, we define the ‘‘subtypes’’ $\{j_\lambda\}$ of a given partition class λ of \mathbf{a} . The partition λ and subtype j_λ determine the value of $T(\mathbf{a}) = T_\lambda(\mathbf{a})$ and $Q(\mathbf{a}) = Q(j_\lambda)$, respectively. We then count the number of elements \mathbf{a} in all partition classes and subtypes, and finally figure out the results.

To be more specific,

$$\begin{aligned} \sum_{\mathbf{a} \in \mathbb{Z}_d^t} Q(\mathbf{a}) T(\mathbf{a}) &= \sum_{\lambda} T_\lambda \sum_{\mathbf{a} \in \lambda} Q(\mathbf{a}) \\ &= \sum_{\lambda} T_\lambda \sum_{(j_\lambda) \in \lambda} \#\{j_\lambda\} Q(j_\lambda). \end{aligned} \quad (\text{F20})$$

For the $X^{(12,13)}$ case, we need to estimate $\sum_{\mathbf{a} \in \mathbb{Z}_d^3} X^{(12,13)}(\mathbf{a}) T(\mathbf{a})$. When $t = 3$, the partition class of \mathbb{Z}_d^3 determines the subsystem weight in \mathbb{Z}_d^3 . We classify the elements by λ and list the values of T_λ and $X^{(12,13)}(j_\lambda)$ in Table I.

Partition classes λ	$\#\{\lambda\}$	T_λ	Subtype $j_\lambda : a^1 a^2 a^3$	$\#\{j_\lambda\}$	$(wt(a^1, a^2), wt(a^1, a^3))$	$X^{(12,13)}(j_\lambda)$
[111]	$1 \times A_d^3$	1	$a b c$	$1 \times A_d^3$	(1, 1)	1
[21]	$3 \times A_d^2$	2	$a a b$ $b a a$	$2 \times A_d^2$ $1 \times A_d^2$	(2, 1) (1, 1)	$-d$ 1
[3]	$1 \times A_d^1$	6	$a a a$	$1 \times A_d^1$	(2, 2)	d^2

TABLE I. The classes and elements number of \mathbf{a} for T_λ and $X^{(12,13)}(j_\lambda)$.

Therefore,

$$\begin{aligned} \sum_{\pi \in S_3} \text{tr}(W_\pi X^{(12,13)}) &= \sum_{\mathbf{a} \in \mathbb{Z}_d^3} X^{(12,13)}(\mathbf{a}) T(\mathbf{a}) \\ &= 1 \times 1 \times A_d^3 + (-d) \times 2 \times 2A_d^2 + 1 \times 2 \times A_d^2 + d^2 \times 6 \times A_d^1 \\ &= 3d^2(d+1). \end{aligned} \quad (\text{F21})$$

For the $X^{\otimes 2}$ case, we need to estimate $\sum_{\mathbf{a} \in \mathbb{Z}_d^4} X^{\otimes 2}(\mathbf{a}) T(\mathbf{a})$. When $t = 4$, the partition class of \mathbb{Z}_d^4 determines the subsystem weight in \mathbb{Z}_d^4 . We classify the elements by λ and list the values of T_λ and $X^{\otimes 2}(j_\lambda)$ in Table II.

Therefore,

$$\begin{aligned} \sum_{\pi \in S_4} \text{tr}(W_\pi X^{\otimes 2}) &= \sum_{\mathbf{a} \in \mathbb{Z}_d^4} X^{\otimes 2}(\mathbf{a}) T(\mathbf{a}) \\ &= 1 \times 1 \times A_d^4 + (-d) \times 2 \times 2A_d^3 + 1 \times 2 \times 4A_d^3 + d^2 \times 4 \times A_d^2 + 1 \times 4 \times 2A_d^2 + (-d) \times 6 \times 4A_d^2 + d^2 \times 24 \times A_d^1 \\ &= d(d+1)(d^2 + 9d + 2). \end{aligned} \quad (\text{F22})$$

□

Partition classes λ	$\#\{\lambda\}$	T_λ	Subtype $j_\lambda : a^1 a^2 a^3 a^4$	$\#\{j_\lambda\}$	$(wt(a^1, a^2), wt(a^3, a^4))$	$X^{\otimes 2}(j_\lambda)$
[1111]	$1 \times A_d^4$	1	$ab cd$	$1 \times A_d^4$	(1, 1)	1
[211]	$6 \times A_d^3$	2	$aa bc$	$2 \times A_d^3$	(2, 1)	$-d$
			$ab ac$	$4 \times A_d^3$	(1, 1)	1
[22]	$3 \times A_d^2$	4	$aa bb$	$1 \times A_d^2$	(2, 2)	d^2
			$ab ab$	$2 \times A_d^2$	(1, 1)	1
[31]	$4 \times A_d^2$	6	$aa ab$	$4 \times A_d^2$	(2, 1)	$-d$
[4]	$1 \times A_d^1$	24	$aa aa$	$1 \times A_d^1$	(2, 2)	d^2

TABLE II. The classes and elements number of \mathbf{a} for T_λ and $X^{\otimes 2}(j_\lambda)$. The sub-type j_λ is determined by the weight of subsystems $a^1 a^2$ and $a^3 a^4$. $\#\{j_\lambda\}$ denote the number of elements contained in the sub-type j_λ .

Appendix G: Concurrence estimation

Concurrence was first proposed as a byproduct of entanglement of formation (EF) [57], and it was proved that for a bi-qubit system, quantum concurrence gives a lower bound for EF. After the proposal of concurrence of bi-qubit systems, many works about how to generalize it to multipartite systems were proposed. In [58], the author defined the quantum concurrence of n -qubit pure state $\Psi \in \mathcal{H}_2^{\otimes n}$ as:

$$C_n(\Psi) = 2^{1-n/2} \sqrt{(2^n - 2) - \sum_i \text{tr} \rho_i^2}, \quad (\text{G1})$$

which is a natural generalization of two-qubit concurrence, where i labels $(2^n - 2)$ nontrivial subsystems and ρ_i is the corresponding density matrix of it. Then the quantum concurrence of multipartite mixed state can be defined as $C_n(\rho) = \inf \sum_i p_i C_n(\Psi_i)$, where the infimum is taken over all pure-state decomposition of ρ , just like the definition of EF. In [76], the author proved that $C_n(\Psi)$ can be measured using just one factorizable observable acting on two identical copies of Ψ :

$$C_N(\Psi) = \sqrt{\langle \Psi | \otimes \langle \Psi | A | \Psi \rangle \otimes | \Psi \rangle}, \quad A = 4(1 - P_1^+ \otimes \dots \otimes P_N^+). \quad (\text{G2})$$

where $P_i^+ = (I_i + S_i)/2$ is the projector that can project states in $\mathcal{H}_i \otimes \mathcal{H}_i$, to symmetric subsystem $\mathcal{H}_i \odot \mathcal{H}_i$. Following this equation, if one wants to estimate $C_N(\Psi)$, he just needs to prepare two identical copies of Ψ and measure observable $P_1^+ \otimes \dots \otimes P_N^+$ on $\Psi^{\otimes 2}$. However, with the help of randomized measurements, $C_N(\Psi)$ can be measured with single copies of Ψ .

Referring to the k -fold twirling channel acting on $X \in \mathcal{H}_2^{\otimes k}$:

$$\Phi^k(X) = \sum_{\pi, \sigma \in \mathcal{S}_k} C_{\pi, \sigma} \text{tr}(X W_\pi) W_\sigma. \quad (\text{G3})$$

Suppose $X = |\psi\rangle\langle\psi|^{\otimes k}$, $|\psi\rangle \in \mathcal{H}_2$, one can easily prove that $\text{tr}(|\psi\rangle\langle\psi|^{\otimes k} W_\pi) = 1, \forall \pi \in \mathcal{S}_k$, so that

$$\Phi^k(|\psi\rangle\langle\psi|^{\otimes k}) = \sum_{\pi, \sigma \in \mathcal{S}_k} C_{\pi, \sigma} W_\sigma = \frac{(d-1)!}{(d+k-1)!} \sum_{\pi \in \mathcal{S}_k} W_\pi. \quad (\text{G4})$$

The second equal sign is because the sum of one row or one column of Weingarten matrix is constant:

$$\sum_{\alpha \in \mathcal{S}_k} Wg_k^{\mathcal{U}_d}(\alpha, \beta) = (d-1)!/(d+k-1)! \quad (\text{G5})$$

where d is the dimension of random unitary and $|\psi\rangle$ in Eq. (G4). According to Eq. (G4), one can generate the projector $P^+ = (I + S)/2$ by two-fold twirling channel

$$\Phi^2 [(|\psi\rangle\langle\psi|)^{\otimes 2}] = \sum_{\pi, \sigma \in \mathcal{S}_2} C_{\pi, \sigma} W_\sigma = \frac{1}{6}(S + I) = \frac{1}{3}P^+. \quad (\text{G6})$$

Recall that virtual operations can be constructed via random evolution and data post processing. According to Eqs. (G2) and (G6), we can design an experimental protocol to measure the quantum concurrence:

Algorithm 4 Concurrence Measurement Protocol

Input: Prepare $|\Psi\rangle$ sequentially for $N_U \times N_M$ times.

Output: Probability distribution of measurement outcomes conditioned on evolution unitary $P(\vec{s}|U)$.

- 1: **for** $i = 1$ **to** N_U **do**
 - 2: Randomly pick a unitary matrix in every unitary ensembles to construct the evolution matrix $U = \bigotimes_{i=1}^n U_i$.
 - 3: Operate U on Ψ to get $U|\Psi\rangle\langle\Psi|U^\dagger$.
 - 4: **for** $j = 1$ **to** N_M **do**
 - 5: Measure $U|\Psi\rangle\langle\Psi|U^\dagger$ in the computational basis $\{|\vec{s}\rangle\}$.
 - 6: Record the measurement results.
 - 7: **end for**
 - 8: Estimate the probabilities $\text{Pr}(\vec{s}, U)$.
 - 9: **end for**
 - 10: Do the data postprocessing given in Eq. (G7) for $C_n(\Psi)$.
-

Then we have

$$C_n(\Psi) = 2\sqrt{1 - 3^n \mathbb{E}_U P(\vec{s}, U)^2} \quad (\text{G7})$$

Proof. Substituting Born's rule and Eq. (G6), one can prove

$$\begin{aligned} 3^n \mathbb{E}_U P(\vec{s}, U)^2 &= 3^n \text{tr} [(|\vec{s}\rangle\langle\vec{s}|)^{\otimes 2} \Phi^{2\otimes n}(\Psi^{\otimes 2})] \\ &= 3^n \text{tr} \{ [\Phi^2(|s_1\rangle\langle s_1|^{\otimes 2}) \otimes \cdots \otimes \Phi^2(|s_n\rangle\langle s_n|^{\otimes 2})] \Psi^{\otimes 2} \} \\ &= \text{tr} [(P_+^1 \otimes \cdots \otimes P_+^n) \Psi^{\otimes 2}] \\ &= \langle \Psi | \langle \Psi | P_+^1 \otimes \cdots \otimes P_+^n | \Psi \rangle | \Psi \rangle, \end{aligned} \quad (\text{G8})$$

so that

$$\begin{aligned} 2\sqrt{1 - 3^n \mathbb{E}_U P(\vec{s}, U)^2} &= 2\sqrt{1 - \langle \Psi | \langle \Psi | P_+^1 \otimes \cdots \otimes P_+^n | \Psi \rangle | \Psi \rangle} \\ &= \sqrt{\langle \Psi | \langle \Psi | A | \Psi \rangle | \Psi \rangle} \\ &= C_n(\Psi). \end{aligned} \quad (\text{G9})$$

□